



1 **In-situ and Denuder Based Measurements of Elemental and Reactive**
2 **Gaseous Mercury with Analysis by Laser-Induced Fluorescence. Results**
3 **from the Reno Atmospheric Mercury Intercomparison Experiment.**

4 Anthony J. Hynes^{*}, Stephanie Everhart, Dieter Bauer, James Remeika, and Cheryl Tatum
5 Ernest¹

6 Division of Marine and Atmospheric Chemistry, Rosenstiel School of Marine and
7 Atmospheric Science, University of Miami, 4600 Rickenbacker Causeway, Miami,
8 Florida 33149.

9 ¹current address: Atmospheric Chemistry Department, Max Planck Institute for
10 Chemistry, Hahn-Meitner-Weg 1, Mainz, 55128, Germany

11 ^{*} Corresponding author. Tel.: +1-305-421-4173; fax: +1-305-421-4689. E-mail address:
12 ahynes@rsmas.miami.edu (A. J. Hynes)

13

14 **Abstract**

15 The University of Miami (UM) deployed a sequential two photon laser-induced fluorescence (2P-LIF)
16 instrument for the in-situ measurement of gaseous elemental mercury, Hg(0), during the Reno Atmospheric
17 Mercury Intercomparison Experiment (RAMIX) campaign. A number of extended sampling experiments,
18 typically lasting 6-8 hours but on one occasion extending to ~24 hours, were conducted allowing the 2P-
19 LIF measurements of Hg(0) concentrations to be compared with two independently operated instruments
20 using gold amalgamation sampling coupled with Cold Vapor Atomic Fluorescence Spectroscopic (CVAFS)
21 analysis. At the highest temporal resolution, ~5 minute samples, the three instruments measured
22 concentrations that agreed to within 10-25%. Measurements of total gaseous mercury (TGM) were made by
23 using pyrolysis to convert total oxidized mercury (TOM) to Hg(0). TOM was then obtained by difference.
24 Variability in the ambient Hg(0) concentration limited our sensitivity for measurement of ambient TOM
25 using this approach. In addition, manually sampled KCl coated annular denuders were deployed and
26 analyzed using thermal dissociation coupled with single photon LIF detection of Hg(0). The TOM
27 measurements obtained were normally consistent with KCl denuder measurements obtained with two
28 Tekran speciation systems and with the manual KCl denuder measurements but with very large uncertainty.
29 They were typically lower than measurements reported by the University of Washington (UW) Detector for
30 Oxidized Hg Species (DOHGS) system. The ability of the 2P-LIF pyrolysis system to measure TGM was
31 demonstrated during one of the manifold HgBr₂ spikes but the results did not agree well with those reported
32 by the DOHGS system. The limitations of the RAMIX experiment and potential improvements that should
33 be implemented in any future mercury instrument intercomparison are discussed. We suggest that
34 instrumental artifacts make a substantial contribution to the discrepancies in the reported measurements



35 over the course of the RAMIX campaign. This suggests that caution should be used in drawing significant
36 implications for the atmospheric cycling of mercury from the RAMIX results.

37
38

39

40 **1.0 Introduction:**

41 The environmental and health impacts of mercury pollution are well recognized with impacts on
42 human health and broader environmental concerns (U.S. EPA., 2000; UNEP, 2013; Mergler et al. 2007;
43 Diez, 2009; Scheuhammer et al., 2007). There have been extensive reviews of global emissions,
44 measurements and biogeochemical cycling of mercury, (Mason, 2009; Streets et al., 2011; Pirrone et al.
45 2009; Lindberg et al., 2007; Ebinghaus et al., 2009; Sprovieri et al., 2010; Selin, 2009) The concerns
46 associated with the mercury problem have resulted in attempts to regulate and control emissions at both
47 national and international levels. The latest attempt in the United States is incorporated in the Mercury and
48 Air Toxics Standards (Houyoux, and Strum, 2011; US EPA, 2013) and international efforts by the United
49 Nations Environment Program have led to the Minamata Convention on Mercury, a global
50 legally binding treaty on mercury controls (UNEP, 2008; UNEP, 2013; UNEP, 2014).
51 There is a reasonable consensus on typical background concentrations of atmospheric mercury, which are
52 extremely low. Currently concentrations range from 1.2–1.4 ng m⁻³ in the Northern Hemisphere and 0.9–
53 1.2 ng m⁻³ in the Southern Hemisphere and appear to be decreasing (Slemr et al., 2011) [1 ng m⁻³ is ~
54 3x10⁶ atoms cm⁻³ or ~ 120 ppq (parts per quadrillion)]. Until recently it has been accepted that most of the
55 mercury found in the boundary layer is elemental mercury, Hg(0) (Lindberg et al., 2007). Oxidized or
56 reactive gaseous mercury (RGM), normally assumed to be in the Hg(II) oxidation state, has not been
57 chemically identified and is thought to constitute a very small fraction of the total mercury concentration
58 although recent work (Gustin et al., 2013, Ambrose et al., 2013) challenges this view. Our overall
59 understanding of the atmospheric chemistry of mercury and the detailed elementary chemical reactions that
60 oxidize Hg(0) is poor (Lin et al., 2006, Hynes et al., 2009; Subir et al., 2012) and the uncertainty of both
61 the chemical identity and measurements of speciated oxidized mercury places few constraints on models.
62 Atmospheric measurements of mercury represent a significant challenge in ultra-trace analytical chemistry
63 and the issues associated with current techniques have been discussed by Gustin and Jaffe (2010). We have
64 developed a laser-based sensor for the detection of Hg(0) using sequential two-photon laser-induced
65 fluorescence (2P-LIF) (Bauer et al., 2002; Bauer et al. 2014). The instrument is capable of fast, in-situ,
66 measurement of Hg(0) at ambient levels. By incorporating pyrolysis to convert RGM and particulate
67 mercury to Hg(0) it is possible to measure total gas phase mercury (TGM) and hence to measure total
68 oxidized mercury (TOM, i.e. the sum of gas phase and particulate bound oxidized mercury) by difference.
69 The Reno Atmospheric Mercury Inter-comparison Experiment (RAMIX) offered an opportunity to deploy
70 the 2P-LIF instrument as part of an informal field intercomparison at the University of Nevada Agricultural
71 Experiment Station (Gustin et al., 2013, Ambrose et al., 2013; Finley et al., 2013). RAMIX was an attempt
72 to inter-compare new Hg measurement systems with two Tekran 2537/1130/1135 systems. This is the



73 instrumentation that is currently in use for the overwhelming majority of atmospheric Hg measurements.
74 Participants included the University of Washington (UW), University of Houston (UH), Desert Research
75 Institute (DRI), University of Nevada Reno (UNR) and the University of Miami (UM). The specific goals
76 for the project were:

- 77 1- Compare ambient measurements of gaseous elemental mercury, Hg(0), gaseous oxidized mercury
78 (RGM) and particulate bound mercury (PBM) by multiple groups for 4 weeks.
- 79 2- Examine the response of all systems to spikes of Hg(0) and HgBr₂.
- 80 3- Examine the response of all systems to Hg(0) in the presence of the potentially interfering
81 compounds ozone and water vapor.
- 82 4- Analyze the data to quantify the level of agreement and the results of interference and calibration
83 tests for each measurement system.

84 In practice the instrument operated by UH only measured Hg(0) for the first week of the campaign and the
85 cavity ring down spectroscopy (CRDS) instrument deployed by DRI did not produce any data. Hence
86 RAMIX was primarily an intercomparison of the UM 2P-LIF instrument, the UW Detector for Oxidized
87 Hg Species (DOHGS) that is based on two Tekran 2537 instruments, and a Tekran 2537 and two
88 2537/1130/1135 speciation systems deployed by UNR. Under these circumstances we were not able to
89 compare 2P-LIF measurements made at high temporal resolution with the CRDS instrument. It did allow us
90 to compare the 2P-LIF sensor with independently operated instruments that use preconcentration on gold
91 coupled with analysis by CVAFS and to examine potential interference effects. Our focus here is to
92 compare the short term variation in GEM on the timescale that the CVAFS instruments operate, ~ 5 minute
93 samples, and examine the ability of the different instruments to capture this variation. In addition, we made
94 measurements of TGM and hence TOM by difference and also employed manual denuder measurements to
95 attempt to measure RGM directly. In prior publications, Gustin et al. (2013) and Ambose et al. (2013)
96 provide their interpretation of the RAMIX results and their conclusions have very significant implications
97 for our understanding of atmospheric mercury chemistry. In this work we offer a contrasting view with
98 different conclusions.

99 2.0 Experimental

100 **2.1 RAMIX Intercomparison.** A detailed description of the RAMIX location and the local meteorology
101 was provided by Gustin et al. (2013). The original RAMIX proposal included participation from Tekran
102 Corporation to build and test a field-deployed, high-flow sampling manifold that could be reliably spiked
103 with 10-100 parts per quadrillion of RGM. Tekran proposed to supply both GOM and GEM spiking using
104 independent generators that were traceable to NIST standards and would be independent of the detection
105 systems being evaluated. However, due to time constraints Tekran believed that it was unlikely that the
106 manifold and ultra-trace spiking system could be manufactured and fully tested to their standards, so they
107 declined to participate in RAMIX (Prestbo, 2016). Instead, the UW group stepped in to supply and operate
108 the sampling manifold and spiking system and the details of its characterization are provided in Finley et al.
109 (2013). During the RAMIX campaign the 2P-LIF instrument sampled on 18 days, typically sampling for



110 between 4 and 6 hours. The longest period of continuous sampling lasted for 26 hours and occurred on
111 September 1st and 2nd. Over this 18 day period we sampled from the RAMIX manifold and, in addition, at
112 the end of the campaign we sampled ambient air independently and also attempted to measure TOM by
113 pyrolyzing the sample air and measuring the difference between Hg(0) and TGM. We also sampled RGM
114 using KCl coated annular denuders using LIF for real-time analysis.

115 **2.2 The 2P-LIF system**

116 Bauer et al. (2002, 2003, 2014) provide a detailed description of the 2P-LIF instrument including
117 the operating principles, linearity tests and examples of experimental data. In summary, the system uses
118 sequential two-photon excitation of two atomic transitions in Hg(0) followed by detection of blue shifted
119 LIF. The instrumental configuration at RAMIX utilized an initial excitation of the Hg 6^3P_1 - 6^1S_0 transition
120 at 253.7 nm, followed by excitation to the 7^1S_0 level via the 7^1S_0 - 6^3P_1 transition at 407.8 nm. Both
121 radiative decay and collisional energy transfer produce population in the 6^1P_1 level. Blue shifted
122 fluorescence was then observed on the strong 6^1P_1 - 6^1S_0 transition at 184.9 nm using a solar blind
123 photomultiplier tube (PMT). By using a solar blind tube that is insensitive to laser scatter at the excitation
124 wavelengths very high sensitivity is possible. The use of narrowband excitation of two atomic transitions
125 followed by detection of laser-induced fluorescence at a third wavelength precludes the detection of any
126 species other than Hg(0). The 2P-LIF instrument requires calibration, so Hg(0) was also measured with a
127 Tekran 2537B using its internal permeation source as an absolute calibration. In prior field campaigns we
128 have been able to transport the Tekran with it remaining powered on which is important in maintaining the
129 stability of the permeation oven. This was not possible during the move from Miami to Reno and so the
130 Tekran was powered down for about one week prior to the start of measurements. We sampled from the
131 RAMIX manifold, which was below ambient pressure, through ~25 ft of ¼ in Teflon tubing. The original
132 RAMIX plan called for all instruments to be located close to the manifold for optimal sampling.
133 Unfortunately the positioning of the trailers at the actual site precluded this and forced us to use a long
134 sampling line. As a result, the internal pump on our Tekran was not able to draw the 2 SLPM required for
135 sampling and an auxiliary pump was placed on the Tekran exhaust to boost the flow.

136 Under atmospheric conditions the 2P-LIF instrument cannot detect RGM so, in principle, this does not
137 need to be removed from the sample gas. However, deposition of RGM on the sampling lines followed by
138 heterogeneous reduction to GEM could produce measurement artifacts. The limit of detection for Hg(0)
139 during RAMIX was ~30 pg m⁻³ for a 10 s or 100 shot average.

140

141 **2.3 Measurements of TGM and TOM**

142 We attempted to use the 2P-LIF instrument to measure TGM and hence TOM by difference. Although we
143 have routinely used this approach to convert HgCl₂ and HgBr₂ to Hg(0) in the laboratory, this was our first
144 attempt to measure total oxidized mercury at ambient concentrations. A second sampling line was attached
145 to the RAMIX manifold and a pyrolyzer was located directly at the manifold sampling port. The pyrolyzer
146 consisted of an ~0.6 cm o.d. quartz tube, 15 cm in length and partially filled with quartz wool. Wrapped



147 Nichrome wire encompassed an 8 cm section of tube that was heated until the quartz began to glow. The
148 high temperature inside the pyrolyzer reduces both RGM and particulate mercury in the manifold air to
149 Hg(0), which is then monitored by 2P- LIF and gives the sum of oxidized (both gaseous and particulate)
150 and elemental mercury, i.e. TGM. Directly sampling from the manifold and measuring ambient Hg(0) then
151 allows the concentration of TOM to be calculated as the difference between the two signals. Sampling was
152 therefore switched between the pyrolyzed and unpyrolyzed sample lines in, typically, 5 min intervals to
153 attempt to track fluctuations in [Hg(0)] that would obscure the relatively small signal increase attributable
154 to TOM.

155 **2.4 Manual Denuder Sampling of RGM**

156 We conducted manual denuder sampling on seven afternoons during the RAMIX campaign to
157 attempt to quantify total RGM, We sampled using both KCl coated annular denuders and uncoated tubular
158 denuders that were then analyzed using programmable thermal dissociation (Ernest et al., 2013). In both
159 cases we monitored the Hg(0) that evolved during RGM decomposition, in real time using single photon
160 LIF. Only the annular denuder results are presented here. The use of denuder sampling coupled with
161 thermal dissociation has been described by Landis et al.(2003) and is used in the Tekran Model 1130
162 Mercury Speciation Units deployed during RAMIX. Air is pulled through a KCl coated annular denuder
163 which captures RGM but transmits elemental and particulate mercury. After a period of sampling, typically
164 one hour, the denuder is flushed with zero grade air and the denuder is heated to 500°C. The RGM is
165 thermally decomposed producing elemental mercury that desorbs from the denuder surface and is then
166 captured and analyzed by a Tekran 2537. The KCl coated annular denuders used here were manufactured
167 by URG Corporation and were identical to those described by Landis et al for manual sampling. They were
168 located on top of one of the RAMIX instrument trailers a few feet from the entrance to the RAMIX
169 manifold inlet. The denuders sampled at 10 SLPM, they were not heated and the integrated
170 elutriator/acceleration jet and impactor/coupler described by Landis et al. and incorporated in the Model
171 1100 speciation unit were not placed on the denuder inlet. Hence no type of particle filtering was used on
172 the inlets. Prior to sampling, the denuders were cleaned by heating to 500 °C and then bagged and taken to
173 the sampling site. After a period of sampling that varied from ~1 to 4 hours, the denuders were capped,
174 placed in sealed plastic bags, and transported to the analysis lab at the University of Nevada, Reno. On
175 most of the sampling days a single denuder was opened and then immediately bagged serving as a field
176 blank. On the final two days of sampling, denuders were sampled in pairs, i.e with two denuders connected
177 inline so that the front denuder sampled RGM and the rear denuder served as a blank and monitor of bleed-
178 through of RGM. The blank concentrations are typically low as shown in Table 1: however on September
179 10th the blank shows a very high value that is indicative of significant contamination at some point during
180 the cleaning or sampling process. For the analysis, a flow of He passed through the denuders and then into
181 a fluorescence cell where any Hg(0) in the flow was detected by LIF. The LIF was monitored by two
182 PMT's set to different gains to increase the dynamic range of the detection system. Prior to the analysis, a
183 known amount of mercury was injected into the flow through a septum using a transfer syringe. The



184 syringe sampled from a Tekran Model 2505 Mercury Vapor Primary Calibration Unit. Without disrupting
185 the gas flow the denuder was then placed in a clamshell tube furnace that had been preheated to 500°C. The
186 evolution of the Hg(0) was monitored for, typically, 5-10 minutes and after the LIF signal had returned to
187 baseline a second calibration injection was performed. A frequency doubled, Nd-Yag pumped dye laser
188 was used to excite the Hg(0) $6^3P_1-6^1S_0$ transition at 253.7 nm and resonance LIF was observed at the same
189 wavelength. In this approach, the detection PMT detects both LIF and laser scatter, hence sensitivity is
190 limited by the ratio of intensity of the LIF signal to the laser scatter. Since the 6^3P_1 level is efficiently
191 quenched by both O₂ and N₂ (Breckenridge and Unemoto, 2007) the thermal analysis was performed in He
192 buffer gas to achieve good detection sensitivity. The excitation beam then passed through a reference cell
193 that contained a steady flow of Hg(0) from a permeation source. The LIF signal from the reference cell
194 served to confirm that the laser output was stable.

195 3.0 Results:

196 3.1 RAMIX Manifold

197 As noted above, the RAMIX manifold had to be constructed and tested by the UW group under tight time
198 constraints. A critique of the manifold performance has been presented by Prestbo (2014) and we detail
199 some key issues here. The manifold deployed at RAMIX was a different size than the prototype tested in
200 the laboratory. The laboratory manifold showed very large variation in calculated transmission efficiencies
201 of GEM after spiking with a permeation source. Recoveries from 71-101% were reported for short-term
202 spikes. The GEM source used for spiking was calibrated by a Tekran 2537B. After the equipment was
203 moved to the RAMIX site the permeation tube output increased. The authors also acknowledge a
204 significant uncertainty ($\pm 15\%$) in the RAMIX manifold flow measurements that were required to calculate
205 spike concentrations; hence this is the minimum uncertainty in calculated spike concentrations.

206 We find that several independent measurements of GEM spikes differ by as much as 30% from
207 the value calculated by the manifold operators suggesting that ($\pm 15\%$) underestimates the uncertainty.
208 Because of these considerations we believe the RAMIX manifold is best treated as a semi-quantitative
209 delivery system and it is most useful to focus on sampling periods when multiple independent instruments
210 show reasonable agreement.

211

212 3.2 UM Tekran Performance

213 In evaluating the first week of the UM RAMIX measurements it became clear that there was some non-
214 linearity in the relative responses of the 2P-LIF and UM Tekran systems and that better agreement was
215 obtained by referencing the Hg(0) concentration to the UNR Tekran. Gustin et al., (2013) concluded that
216 the UNR Tekran, based on the inlet configuration, only measured Hg(0) and they suggested that the UM
217 system, due to the long sampling line, was measuring TGM. We compared the manifold Hg(0) readings
218 from the UM and UNR Tekrans over the first 260 hours in which we took measurements. The absolute
219 concentration difference relative to the UNR instrument is shown in Figure 1. Hour zero corresponds to 9
220 am on August 26th when we started measurements and hour 260 corresponds to midnight on September 5th.



221 Over the first 24 hours the UM Tekran is offset by $\sim 0.5 \text{ ng m}^{-3}$ and then jumps to $\sim 2 \text{ ng m}^{-3}$ at hour 30 on
222 August 27th with the difference decreasing over the next week of measurements in an almost linear fashion.
223 Over most of this period the UW Tekran did not report Hg(0) measurements other than a small set of
224 measurements on August 28th that are offset by $\sim 0.5 \text{ ng m}^{-3}$ relative to the UNR Tekran. It can be seen that
225 by hour 250 on September 5th all three instruments had converged. After this period the agreement between
226 the UNR and UM Tekrans was good until September 8th, when the UM instrument became contaminated
227 after a malfunction of our permeation oven, requiring replacement with a backup Tekran 2537A unit. We
228 conclude that the difference between the UM and UNR instruments is likely to be an experimental artifact
229 possibly associated with the fact that the UM instrument had been powered down for almost one week and
230 relocated to a site at a significantly different ambient pressure. The initial abrupt change to a large offset
231 followed by the linear decrease over 300 hours cannot, in our view, be caused by any type of chemistry
232 within the manifold, nor can it be indicative of the UM instrument measuring TGM rather than Hg(0).
233

234 3.3 2P-LIF Measurements

235 The absolute Hg(0) concentrations reported for the 2P-LIF measurements typically use a single 10-minute
236 section of Tekran concentration data to calibrate the 2P-LIF signal and place it on an absolute concentration
237 scale. The complete time series of measurements then gives a long-term comparison of the 2P-LIF and
238 Tekran instrumentation with the absolute 2P-LIF concentrations based on the single 10-minute calibration
239 point.
240

241 3.3.1 September 5th

242 This was the first occasion on which the three independent Tekran 2537 instruments and the 2P-
243 LIF system reported simultaneous measurements. The 2P-LIF system sampled from the RAMIX manifold
244 for approximately 6.5 hours from $\sim 10:30 \text{ am}$ to 5 pm. Over the course of the sampling period there were
245 two spikes of Hg(0) lasting one and two hours, respectively. The UW manifold team reported an initial 10
246 am Hg(0) spike concentration of 26.5 ng m^{-3} dropping to 24.4 ng m^{-3} over the course of the one hour spike.
247 The two hour spike that began at 1 pm was reported to be $\sim 12.4 \text{ ng m}^{-3}$ dropping to 10.5 ng m^{-3} over the
248 course of two hours. The ambient airflow in the manifold was spiked with HgBr₂ for the whole of this
249 sampling period and the reported level of the HgBr₂ spike varied between 0.6-0.7 ng m^{-3} . The levels of
250 HgBr₂ measured by the DOHGS instrument were consistent with this but the concentrations reported by the
251 UNR speciation units were considerably lower and with a significant discrepancy between the two
252 speciation units. Figure 2a shows the sequence of Hg(0) measurements from the UNR, UW and UM
253 Tekrans together with the 5 minute averages of the 2P-LIF signal. The 2P-LIF instrument began manifold
254 measurements in the middle of the initial 10 am Hg(0) spike and is scaled to the concentration at this time
255 which all three Tekrans measured as $\sim 22.5 \text{ ng m}^{-3}$. The three Tekrans agree to better than 5% during both
256 of the manifold spikes and, based on a pre-spike ambient concentration of 2 ng m^{-3} it suggests that the
257 initial spike concentration was $\sim 20.5 \text{ ng m}^{-3}$. This suggests that the reported spike concentration was ~ 25 -



258 30% larger than the actual concentration introduced into the manifold. Fig. 2b shows an expanded
259 concentration scale to highlight the nominally ambient measurements. There is some suggestion that it took
260 some time for the spike to be completely removed, particularly after the second spike. At the completion of
261 the second spike all the instruments drop to ambient but the UNR instrument sees two Hg(0) “pulses”.
262 Interestingly these show up with greatly reduced amplitudes in the UW and UM Tekran signals and also in
263 the 2P-LIF signal. Figure 3 shows the % difference of the other instruments relative to the UM Tekran and
264 over most of the sampling period the agreement between all the measurements is better than 10% over an ~
265 7 hour period with 5 minute sampling resolution. This indicates that the 2P-LIF instrument is capable of
266 stable operation over an extended time period with any drifts being corrected by normalization to the
267 reference cell. Well calibrated independently operated Tekrans should be capable of agreement to better
268 than 5% based on tests performed by the manufacturer and this level of agreement is achieved during
269 subsets of the sampling period. It is not clear if the deviations that are observed, particularly the large
270 deviations seen by the UNR Tekran after the second spike are related to presence of elevated levels of
271 HgBr₂, or other issues related to manifold operation. The fact that all the instruments observed these Hg(0)
272 pulses suggests that the artifact may be related to a process in the manifold rather than in in the UNR
273 sampling line. However the significant differences in the magnitude of Hg(0) pulses observed by the
274 different instruments are difficult to rationalize.

275

276 3.3.2 September 1st and 2nd

277 The UM and UNR systems sampled simultaneously for a 22 hour period offering an opportunity to
278 compare the instruments over an extended sampling period. This sampling also occurred prior to any of the
279 manifold spikes that introduced substantial concentrations of HgBr₂ into the manifold and sampling lines.
280 Unfortunately, the UW instrument did not report any measurements during this sampling period. The UM
281 system sampled for 26 hours and the complete dataset is described elsewhere, (Bauer et al. 2014). This
282 includes a detailed analysis of the short-term, i.e. 1-10 seconds, variation in the Hg(0) concentration and the
283 ability of the 2P-LIF system to capture this. Here we focus on the simultaneous sampling period and the
284 variability that should be resolvable by both of the Tekrans and the 2P-LIF instruments. SI Figure 1 shows
285 the 24 hour sampling period with the 2P-LIF signal calibrated by the UM Tekran concentration at the
286 beginning of hour 13 (i.e. 1 pm on September 1st) and the corresponding measurements from the UNR
287 Tekran. SI Figure 2 shows the same data with an expanded y-axis to highlight the variation in the ambient
288 measurements. All three instruments track each other quite well over the first 10 hours and then measure a
289 nocturnal increase in Hg(0) which shows greater medium term variability in the concentration. The 2P-LIF
290 concentrations are approximately 20% greater than the Tekran measurements during this period. At hour 33
291 (i.e. 9 am on September 2nd) there was a manifold spike with a reported concentration of 12.9 ng m⁻³
292 dropping to 11.9 ng m⁻³ over the course of one hour. The UNR Tekran is ~6% lower, the UM Tekran is
293 ~20% lower and the 2P-LIF ~22% higher than the calculated spike concentration. SI Figure 3 shows the
294 same measurement set but with all instruments normalized to the second manifold spike at hour 33. Figure



295 4 shows an expanded y-axis, the concentration scale, focusing on the ambient concentration measurements.
296 It is apparent that we now see better agreement between the 2P-LIF and the UNR Tekran but that the UM
297 Tekran lies systematically higher than the UNR Tekran. Figure 5 shows a three hour subset of the
298 measurements corresponding to 5-8 am on the morning of September 2nd. The variation between the
299 instruments is greater than 5% and the short term variations in the Hg(0) concentration vary between the
300 three instruments. Using either calibration approach we see that all instruments capture both the nocturnal
301 increase in Hg(0) concentration and the greater variability in the signal but that there are differences in the
302 amplitude of the variability.

303

304 3.3.3 Hg(0) Intercomparison Conclusions

305 Almost all of the measurements of atmospheric concentrations of Hg(0) have been made with
306 CVAFS instrumentation and the majority of those measurements have utilized the Tekran 2537. This work
307 provides the first extensive comparison of the Tekran 2537 with an instrument that is capable of fast in-situ
308 detection of Hg(0) using a completely different measurement technique. Measurements over two extended
309 sampling periods show substantial agreement between the 2P-LIF and Tekran measurements and suggest
310 that all the instruments are primarily measuring the same species. Intercomparison precision of better than
311 25% was achievable over an extended sampling period and precision of better than 10% was achieved for
312 subsets of the sampling period. As we discuss below it is difficult to determine the extent to which
313 interferences from GOM contribute to the differences observed.

314

315 3.4 Interference Tests.

316 As noted above, one component of the initial RAMIX proposal was an examination of the response of the
317 various sensors to potential interfering compounds HgBr₂, O₃ and H₂O. An analysis of the 2P-LIF
318 detection approach suggests that, at the spike levels employed during the RAMIX campaign, neither HgBr₂
319 nor O₃ should have any interference effects. Changes in the concentration of H₂O do affect the 2P-LIF
320 signal because H₂O absorbs the 2P-LIF fluorescence signal and may quench the fluorescence. In addition,
321 O₂ also absorbs the 2P-LIF signal and quenches fluorescence thus a change in the O₂ concentration will
322 affect the linearity of the response. We have presented a detailed discussion of these effects (Bauer et al.,
323 2014) including an examination of two types of interferences that have been observed in LIF sensors
324 applied in atmospheric and combustion environments and concluded that these are not potential problems
325 in 2P-LIF measurements of atmospheric Hg(0). As we have noted previously (Bauer et al., 2014),
326 condensation in our sampling lines can produce artifacts in Hg(0) concentration measurements. Because of
327 the low humidity in Reno it was not necessary to use any type of cold trap during ambient measurements
328 but we did use a trap during manifold spikes of H₂O so our measurements do not address this as a potential
329 interference.

330 3.4.1 O₃ Interference Tests.



331 On September 7th an ozone interference test was conducted by simultaneously spiking the
332 sampling manifold with a high concentrations of Hg(0) and ozone. The spike in Hg(0) lasted from 9am to
333 7:30 pm and there were two ozone spikes, each of two hours duration. A comparison of the UM, UW and
334 UNR Tekrans and the 2P-LIF signal is shown in Figure 6. The UW Tekran only measured for a portion of
335 this period but agrees reasonably well with the other Tekrans. The 2P-LF signal is calibrated by the UM
336 Tekran reading during the initial Hg(0) spike at hour 9.30. The 2P-LIF signal was online for 6 minutes at
337 the beginning of the first ozone spike and then went offline for ~40 minutes for instrument adjustments.
338 When the 2P-LIF came back online the magnitude of the normalized signal was low relative to the Tekrans.
339 At hour 13 all three instruments converge and agree well over the course of the second spike. The
340 magnitude of the 2P-LIF signal could have been affected adversely by the adjustments but any reduction in
341 signal should have been compensated by a corresponding change in the reference cell. The elevated levels
342 of ozone were introduced into the manifold by UV irradiation of O₂ and adding the O₂/O₃ gas mixture
343 directly into the manifold produced a reported ~8% relative increase of O₂ levels in the manifold mixing
344 ratio. As we note above this additional O₂ would absorb some of the 2P-LIF signal but this would be a very
345 small effect. The enhanced quenching by O₂ is more difficult to assess but cannot explain the discrepancy
346 between the Tekrans and the 2P-LIF signal. In addition the agreement during the second ozone spike was
347 good. One possible explanation is that the increase in the O₂ mixing ratio was larger than calculated for the
348 first spike. A second series of O₃ spikes were conducted on September 13th when we were attempting to
349 measure total gaseous mercury using pyrolysis as described below. The 2P-LIF measurements switched on
350 a five-minute cycle between a pyrolyzed line that would have decomposed all the ozone in the sample and
351 a line containing the ambient air spiked with ozone. There was no difference in the 2P-LIF signal from the
352 two sampling channels again suggesting that O₃ has no interference effects. The changes in the Hg(0)
353 concentration measurements track the predicted changes in calculated spike concentration. However the
354 calculated spike concentration is 20-40% higher than the actual measurements obtained by the UM Tekran.
355

356 3.5 Measurements of TGM and TOM

357 We made attempts to use the 2P-LIF instrument to measure TGM and hence TOM by difference by
358 sampling through two manifold lines. A pyrolyzer was located at the manifold on one of the sampling lines
359 to measure TGM. The other sampling line measured ambient Hg(0). TOM was calculated from the
360 difference in the TGM and Hg(0) concentrations and in this sampling configuration the limit of detection
361 for TOM depends on the short term variability in ambient Hg(0) which is significant and shows a diurnal
362 variation. The pyrolysis system was set up and tested on September 12. Manifold sampling was conducted
363 on the 13th and 14th and sampling from the trailer roof occurred on the 15th. We calculated the means of the
364 pyrolysis and ambient channel concentrations, and the difference which gives the TOM concentration. We
365 also calculated the standard deviations and standard errors (SE) and used these errors to calculate in
366 quadrature the 2SE uncertainty in the derived TOM concentration. However, as discussed below, the errors
367 in the means do not appear to capture the full variability in Hg(0), particularly at shorter sampling times.



368 3.5.1 September 14th

369 Our most extensive sampling took place on the 14th and we were able to sample for three ~ 2 hour periods
370 between 9 am and 8 pm. On this day there were multiple manifold spikes of HgBr₂ and also an Hg(0) spike
371 and we have made a detailed analysis of the data for each sampling period.

372 The third sampling period which included a large HgBr₂ spike provided the only definitive
373 opportunity to demonstrate the capability of 2P-LIF coupled with pyrolysis to measure oxidized mercury.
374 The third sampling period began at ~ hour 17.3 during a manifold HgBr₂ spike that began at hour 17. A
375 short Hg(0) spike was also introduced at hour 18. Fig. 7 shows the 2P-LIF signals from the ambient and
376 pyrolyzed sampling lines together with the means and 1 standard deviation. The UM Tekran was offline at
377 this time and so the 2P-LIF concentrations are calibrated by the concentrations reported by the UNR
378 Tekran at the beginning of the Hg(0) spike which are also shown. Both the UNR Tekran and UW Tekran
379 report very similar Hg(0) concentrations during the Hg(0) spike. Both systems report an Hg(0)
380 concentration of 6.7 ng m⁻³ at the beginning of the spike which, since the pre-spike concentration was ~1.9
381 ng m⁻³, corresponds to a spike concentration of 4.8 ng m⁻³. This is lower than the calculated spike
382 concentration of 6.1 ng m⁻³ reported by the manifold operators and suggests that the calculated spike was
383 ~27% higher than the actual spike concentration introduced into the manifold. Fig. 8 shows the means of
384 each set of ambient and pyrolyzed measurements together with the 2σ variation and 2SE of the mean. Fig. 9
385 shows the TOM concentrations calculated from the difference together with 2SE in the TOM concentration.
386 The reported spike concentrations and DOHGS measurements are also shown. During the initial sampling
387 period between ~17.3- 17.8 hours the 2P-LIF pyrolysis measurements do not show evidence for an HgBr₂
388 spike. Taking the difference between the ambient and pyrolyzed measurements during this period we obtain
389 [TOM] = 0.05±0.05 ng m⁻³. Shortly before the introduction of the Hg(0) spike we see clear evidence for an
390 increase in the Hg(0) concentration in the pyrolysis sample relative to the ambient sample. We speculate
391 that the manifold adjustments that were made to introduce the additional Hg(0) spike produced either a
392 change in the flow or some other change in the manifold conditions that allowed the HgBr₂ spike to reach
393 our pyrolyzer, which, as mentioned above, was located at the manifold. This difference between the two
394 2P-LIF signals is clearly evident by inspection of Fig.7. The TOM concentration which should consist
395 almost exclusively of HgBr₂ is significantly larger than both the reported HgBr₂ spike concentration and the
396 concentrations reported by the DOHGS system which are in perfect agreement. Taking the difference
397 between the ambient and pyrolyzed measurements for hour 18.02-18.35 we obtain [TOM] = 1.20±0.17 ng
398 m⁻³ with 2SE uncertainty. It is important to note again that the calculated Hg(0) concentration is 27% larger
399 than the measured concentration. This large difference is most likely due to errors in the flows or the
400 permeation source output but it suggests significant uncertainty in the calculated concentration of the
401 HgBr₂ spike. In addition, it is clear that the DOHGS measurements show a different temporal profile of
402 TOM. The DOHGS system reports TOM concentrations that agree almost exactly with the calculated spike
403 concentration, at the beginning of the spike period and drop to a very low background level that is below
404 the detection limit at the end of the reported spike period. In contrast, the 2P-LIF measurements do not



405 show an increased TOM concentration until shortly before the introduction of the Hg(0) spike and they take
406 ~20 minutes to drop to background levels. The UNR speciation systems sample for 1 hour and this is
407 followed by a 1 hour analysis period so they produce a single hourly average every two hours. During this
408 period the UNR speciation system Spec1 sampled for ~ 20 minutes during the spike period and then for a
409 further 40 minutes. Spec2 was sampling ambient air outside the manifold.

410 SI Figure 4 shows the 7s average of the 2P-LIF signal from the ambient and pyrolysis sample lines
411 for the first sampling period 8-10.45 hours together with the mean and 1 standard deviation (1σ) variation
412 in the 2P-LIF signals. SI 5 shows the means together with the 2σ variation and 2SE of the mean. It is clear
413 that there is significant short term variability in the ambient Hg(0) concentration. SI Fig. 6 shows the TOM
414 concentrations calculated from the difference between the pyrolyzed and ambient channels together with
415 the calculated 2SE in the TOM concentration. The reported spike concentration and DOHGS concentration
416 measurements are also shown. If we take the means of the 2P-LIF ambient and pyrolysis measurements
417 during the reported spike period we obtain: ambient: 2.06 ± 0.05 ng m⁻³ and pyrolyzed: 2.21 ± 0.03 ng m⁻³
418 giving a TOM concentration of 0.145 ± 0.05 ng m⁻³. The 2P-LIF measurements are consistent with the
419 detection of TOM but they are much lower than the calculated spike and DOHGS measurements.

420 SI Figs. 7-9 show the corresponding plots for the second sampling period from ~ 12.2-14 hours.
421 The alternating sampling between the ambient and pyrolysis channels is more even and SI Fig. 7 shows that
422 there is still variability in ambient Hg(0). The means of all the samples give: ambient: 1.72 ± 0.02 ng m⁻³,
423 pyrolyzed: 1.70 ± 0.02 ng m⁻³. If we take the subset of measurements that coincide with the reported spike
424 we obtain: ambient: 1.79 ± 0.02 ng m⁻³ pyrolyzed 1.77 ± 0.02 ng m⁻³. In this case, the 2P-LIF measurements
425 do not detect HgBr₂ and are not consistent with the reported spike or DOHGS measurements.

426 SI Figs. 10 and 11 show the averages of the TOM concentrations from the 2P-LIF system together
427 with the measurements from the UNR speciation systems, the reported spike concentrations and 5 min
428 DOHGS concentrations. During this sampling period Spec1 sampled from the RAMIX manifold while
429 Spec2 sampled ambient air outside the manifold. Gustin et al.(2013) detail problems with the response of
430 the Spec2 system and applied a 70% correction that is also shown as "Spec2 corrected". Because both the
431 DOHGS and 2P-LIF pyrolysis systems are expected to measure the sum of gaseous (RGM) and particulate
432 (PBM) oxidized mercury we have plotted the sum of the RGM and PBM concentrations from the
433 speciation systems. They are plotted at the mid-point of the 1 hour sampling period.

434 Over most of the measurement period the 2P-LIF pyrolysis and Spec1 measurements are
435 consistent and lower than the DOHGS measurements. The exception is the large spike in TOM seen by the
436 2P-LIF system at hour 18. The spike occurred during the initial portion of Spec1 sampling and, although it
437 measures an increase in RGM relative to Spec2, the magnitude is not consistent with the 2P-LIF pyrolysis
438 observations.

439

440 **3.5.2 September 13th**



441 September 13th was the first day we were able to sample with the pyrolysis system and we sampled over a
442 period of 5 hours. The only manifold spike during this period was an O₃ spike at 1 pm that lasted one hour
443 so the speciation instruments were attempting to measure ambient RGM. SI Figure 12 shows averages of
444 TOM concentrations as measured by the 2P-LIF pyrolysis system together with the hourly averages as
445 measured by DOHGS and UNR speciation instruments. The x-axis error shows the duration of the 2P-LIF
446 measurements together with 2SE y-axis error bars. Two of the averages of the 2P-LIF measurement give a
447 physically unrealistic negative concentration suggesting that combining the 2SE errors in the means of the
448 ambient and pyrolyzed channels underestimates the uncertainty in the TOM measurement.

449 3.5.3 September 15th.

450 On September 15th we sampled from the trailer roof using the same sampling lines and again
451 alternating between the pyrolyzed and unpyrolyzed channels. SI Figure 13 shows the averages of the 2P-
452 LIF signal from the ambient and pyrolysis channels together with the concentrations measured by the
453 Spec2 system that was sampling ambient air outside the manifold. The concentration obtained from the UM
454 denuder samples described below are also shown. The UW DOHGS and Spec1 systems were sampling
455 from the RAMIX manifold with continuous HgBr₂ spiking during this period. We see some evidence for
456 measurable RGM in the first hour of the measurements and this is not seen by Spec 2. Later measurements
457 show no evidence for measurable RGM concentrations.

458 3.6 Limits of 2P-LIF detection of TOM

459 As we have noted above, the limit of our detection of TOM depends on the short term variability
460 in the ambient Hg(0) concentration because we use a single fluorescence cell and switch between pyrolysis
461 and ambient channels. We have attempted to give an estimate of the uncertainty by taking two standard
462 errors of the means and combining the errors in quadrature to get an estimate of the uncertainty in the TOM
463 concentration. If the mean of the ambient Hg(0) concentration is not fluctuating significantly on the
464 timescale of channel switching this approach should give an accurate estimate of the uncertainty in TOM.
465 In fact our Hg(0) observations show that the fluctuations in the Hg(0) concentration show a significant
466 diurnal variation, with large fluctuations at night, decreasing over the course of morning hours and being
467 smallest in the afternoon. This can be seen in the long term sampling from September 1st and 2nd and in the
468 observations from September 14th. The observation of statistically significant but physically unrealistic
469 negative TOM concentrations on September 13th may be explained by this. Such an artifact could be
470 produced by contamination in the Teflon valve switching system that alternates the flow to the fluorescence
471 cell. This type of contamination should produce a constant bias that is not actually observed. It appears that
472 the short term variability in Hg(0) concentration produces a small bias in some cases that is not averaged
473 out by switching between the ambient and pyrolyzed channels. For example on September 13th the initial
474 sample period of 1.2 hours gives an RGM concentration of $0.06 \pm 0.10 \text{ ng m}^{-3}$ while two shorter sampling
475 periods at hour 10.5 (36 min sample) and 13.5 (12 min sample) give $0.15 \pm 0.09 \text{ ng m}^{-3}$. Our results suggest
476 that the use of single detection channel with switching between ambient and pyrolyzed samples is not
477 adequate to resolve the small concentration differences that are necessary to be able to monitor ambient



478 TOM. It is necessary to set up two detection systems, one continuously monitoring ambient Hg(0) and the
479 other continuously monitoring a pyrolyzed sample stream giving TGM, to get the precision necessary to
480 monitor ambient TOM. Over most of the measurement periods our results are consistent with the lower
481 TOM values reported by the UNR speciation instruments although there is a large uncertainty in the
482 concentrations that is actually difficult to quantify. In addition, it is important to emphasize that this was
483 our first attempt to use the pyrolysis approach to attempt to measure TOM. It is possible that the pyrolyzer
484 was not working efficiently on September 13th. The results from September 14th are more difficult to
485 rationalize. The 2P-LIF pyrolysis system has the sensitivity to detect the much higher values of RGM
486 reported by the DOHGS system and the reported spike concentrations of HgBr₂. At higher concentrations,
487 as shown in Fig. 9, the 2P-LIF system can monitor HgBr₂ with ~10 minute time resolution. Our results,
488 however, cannot be reconciled with those reported by the DOHGS system or the spike concentrations
489 reported by the UW manifold team.

490

491 3.7 Manual Denuder Measurements:

492 As we describe above, our use of manual denuders is similar to that described by Landis et al. (2002) with
493 the exception that we do not incorporate the integrated elutriator/acceleration jet and impactor/coupler on
494 the denuder inlet. Feng et al. (2004) suggested that such impactors could reduce the efficiency of RGM
495 collection. Hence no type of particle filtering was used on the inlets. In addition, we used single photon LIF
496 to monitor the evolution of Hg(0) in real-time as the RGM decomposed on the hot denuder surface during
497 oven analysis. The analysis was carried out in He buffer gas and the Hg(0) concentration was calibrated by
498 manual injections. The first series of measurements, i.e. September 6-14th involved single denuder
499 sampling. On the 15 and 16th we employed tandem sampling with two denuders in series to assess the
500 extent of RGM “bleedthrough”. We used two sets of denuders on the 15th and four sets of denuders on the
501 16th. Fig. 10 shows the raw data for a denuder analysis showing the preheat Hg(0) calibration injections and
502 the temporal profile of the Hg(0) LIF signal for one of the September 16th samples, denuder 1. The two
503 traces correspond to the two monitoring PMTs set at different gains to increase the dynamic range of the
504 measurements. Fig. 11 shows the calibrated profile for the same denuder together with the “blank” i.e. the
505 trailing denuder. The complete set of manual denuder data together with corresponding values for the UNR
506 speciation units that are closest in sampling time are shown in Table 1. Sampling occurred on denuders 1,
507 4, 6 and 7. The “trailing” denuders which we have treated as blanks, are denuders 3, 5, 8 and 9. The
508 advantage of monitoring the RGM decomposition in real-time is shown in the September 16th data. The
509 temporal decomposition profiles (TDP) for three of the denuders shown in Fig 11 and SI Figures 14 and 15
510 show reasonable agreement both in absolute concentration of Hg(0) and the time for decomposition to
511 occur. The fourth denuder sample, SI Fig. 16, is a factor of 4-5 higher in concentration and decomposes on
512 a longer time scale with significant structure in the TDP. Comparing the TDPs for all eight denuders it is
513 clear that the TDP for denuder 7, which shows the anomalously high value, is very different from the TDPs
514 for the other three sample denuders. We believe that this TDP is associated with particulate mercury that



515 has impacted on the denuder wall and decomposes on a slower timescale giving a very different temporal
516 profile from RGM that was deposited on the denuder wall. SI Table 1 shows the values of RGM obtained
517 from denuder analysis together with an indication of impact from a PBM component. We have also
518 included measurements from the UNR speciation systems that overlap with, or are close to, the times when
519 our measurements were made. We draw several conclusions from the measurements. The values we obtain
520 from simultaneous measurements that are not influenced by the presence of PBM agree reasonably well
521 with each other, are broadly consistent with the values reported by the Tekran speciation systems and are
522 typically much lower than the values from the UW DOHGS system. Two sets of tandem denuder
523 measurements from September 15 and 16 indicate that there is not a significant level of “bleedthrough”
524 onto the trailing denuders. This suggests that the large differences between the DOHGS system and the
525 UNR speciation systems are not due to specific problems with the RAMIX manifold or the speciation
526 systems deployed at RAMIX even though Spec 2 was not functioning properly as documented by Gustin et
527 al. (2013). The tandem sampling also demonstrates that any denuder artifact is not a result of some type of
528 “bleedthrough” artifact that is preventing RGM from being quantitatively captured by the first denuder. It is
529 also noteworthy that the manually sampled denuders were at ambient temperature in contrast to the
530 speciation denuders that are held at 50 C. Hence the absolute sampling humidities are similar but the
531 relative humidities are very different. Finally, we suggest that there is value in monitoring RGM
532 decomposition in real time as diagnostic of particulate impact when utilizing the annular denuders without
533 the impactor inlet designed to remove coarse particulate matter that may be retained due to gravitational
534 settling

535 **4.0 Implications of RAMIX results.**

536 We think a realistic assessment of the RAMIX results is imperative because the interpretation of
537 the RAMIX data and the conclusions presented by Gustin et al. (2013) and Ambrose et al. (2013) have
538 enormous implications for both our understanding of current experimental approaches to atmospheric
539 sampling of mercury species and to the chemistry itself. Speciation systems using KCl denuder sampling
540 are widely used in mercury monitoring networks worldwide to measure RGM concentrations and the
541 Gustin et al. (2013) and Ambrose et al. (2013) papers suggests these results greatly underestimate RGM
542 concentrations with no clear way to assess the degree of bias.

543 **4.1 Intercomparison of Hg(0)**

544 The assessment of the Hg(0) measurements is a little different in the two manuscripts with
545 Ambrose et al. (2013), noting that “comparisons between the DOHGS and participating Hg instruments
546 demonstrate good agreement for GEM” they found a mean spike recovery of 86% for the DOHGS
547 measurements of GEM, based on comparisons between measured and calculated spike concentrations.
548 Gustin et al. (2013) suggest that the UM Tekran agreed well with measurements of TM reported by the
549 DOHGS system and they “hypothesize that the long exposed Teflon line connected to the UM Tekran unit
550 provided a setting that promoted conversion of RM to GEM, or that RM was transported efficiently through
551 this line and quantified by the Tekran system. The latter seems unlikely given the system configuration...”,



552 where RM refers to reactive mercury. As we note above, we believe that the best explanation for
553 discrepancies between the UM and UNR Tekrans is an experimental issue with the UM Tekran response
554 during the initial period of sampling. We would suggest that data from September 5th, one of the few
555 occasions when data from multiple instruments agreed over an extended period is not compatible with
556 either transmission or inline reduction of RGM in our sampling line. What is also significant from this data
557 is the very large discrepancy between the spike concentrations as measured independently by three
558 different Tekran systems and confirmed by the relative response of the 2P-LIF measurements and the
559 calculated spike concentration. The discrepancy, on the order of 25-30%, is larger than the manifold
560 uncertainties suggested by Finley et al. (2013). We note other examples of the measured Hg(0) spikes
561 being significantly lower than the calculated concentrations. In prior work we have shown that both the
562 Tekran and 2P-LIF systems show excellent agreement over more than 3 orders of magnitude in
563 concentration when monitoring the variation in Hg(0) in an N₂ diluent. It is to be expected therefore that the
564 “recovery” of high concentration spikes should show good agreement between the different instruments as
565 observed in the September 5th data. The difference between the observations and the calculated manifold
566 spike concentrations is, we would suggest, a reflection of the significant uncertainty in the calculated
567 manifold spike concentration and is not a reflection of reactive chemistry removing Hg(0). In addition,
568 random uncertainties in the flow calculations should not produce a consistently low bias relative to the
569 calculated spike concentrations. As we note above in section 3.1 Ambrose et al. report an increase in the
570 output of their Hg(0) permeation tube after the move to the RAMIX site but this assumes that their Tekran
571 calibration is accurate. The results are consistent with their Tekran measuring too high an output from the
572 permeation device. This is significant if the same Tekran is being used to calibrate the output of the HgBr₂.

573 A more difficult issue is the question of resolving the differences in the temporal variation of
574 ambient Hg(0) at the 5 minute timescale as captured by the different instruments. The Tekran systems
575 should be in agreement with a precision of better than 5% and the 2P-LIF system, with a much faster
576 temporal resolution and detection limit, should be capable of matching this. The differences here are not
577 consistently associated with a single instrument with, for example, the 2P-LIF having some systematic
578 offset with respect to the CVAFS systems. The extent to which the larger (i.e. larger than 5%) observed
579 discrepancy which ranged from 10% to 25% is a result of interferences or simply a reflection of instrument
580 precision is difficult to assess. We note again that the UM instruments had to sample through a very long
581 sampling line and we expect that oxidized mercury is deposited on the sampling line. However it is not
582 possible to assess the extent to which oxidized mercury is reduced back to its elemental form introducing
583 small artifacts. As we suggest below, an intercomparison of instrument response to variation in Hg(0)
584 concentrations in a pure N₂ diluent with the Hg(0) concentration varying between 1-3 ng m⁻³ would provide
585 a definitive baseline measurement of the instrument intercomparison precision and accuracy. We suggest
586 that such a measurement is a critical component of any future intercomparison of mercury instrumentation.

587

588 4.2 Comparison of Total Oxidized Mercury



589 To the best of our knowledge RAMIX is the only experiment that has measured ambient TOM using
590 multiple independent techniques. It should again be emphasized that the TOM measurements using
591 pyrolysis with 2P-LIF detection were the first attempt to perform such measurements and the use of a
592 single channel detection system introduced large uncertainties into the measurements. The very large
593 discrepancies between the measurements of TOM reported by the DOHGS system, the Tekran speciation
594 systems and the limited number of 2P-LIF pyrolyzer measurements are the most problematic aspect of the
595 RAMIX measurement suite. Work prior to RAMIX and suggested a potential ozone and/or humidity
596 interference in the operation of KCl coated annular denuders and a number of studies since have also
597 reported such an effect (Lyman et al., 2010; McClure et al., 2014). Typically however the differences
598 between the RAMIX measurements are large and are not germane to the differences between the DOHGS
599 and 2P-LIF pyrolyzer measurements. The SI Figures give an example of the differences between the
600 DOHGS measurements and the denuder and 2P-LIF measurements. Ambose et al. (2013) note that the
601 DOHGS measurements were, on average, 3.5 times larger than those reported by the Spec1 system and
602 summarize the comparison with denuder measurements as follows: “These comparisons demonstrate that
603 the DOHGS instrument usually measured RM concentrations that were much higher than, and weakly
604 correlated with those measured by the Tekran Hg speciation systems, both in ambient air and during HgBr₂
605 spiking tests.” The discrepancy of a factor of 3.5 is an average value but, for example, examining the
606 September 14 data at ~5 am the DOHGS system is measuring in excess of 500 pg m⁻³ compared with ~20
607 pg m⁻³ measured by the speciation systems, a factor of 25 difference. At this point the Hg(0) concentration
608 was ~ 3 ng m⁻³ so based on the DOHGS measurements oxidized mercury is ~ 15% of the total mercury
609 concentration. A recent study by McClure et al. (2014) provided a quantitative assessment of the extent to
610 which ozone and humidity impact the recovery of HgBr₂ on KCl recovery. They note that although they
611 provide a recovery equation to compare with other studies, they do not recommend use of this equation to
612 correct ambient data until more calibration results become available. In Fig 12, we show the ozone
613 concentration and absolute humidity for a 35 hour sampling period on September 13th and 14th that included
614 two ozone spikes and only sampled ambient TOM. Fig 13 shows the expected denuder recovery based on
615 the formula determined by McClure et al. which varies between a typical value of ~70% dropping to ~50%
616 during the ozone spikes. The figure also shows the reported recoveries i.e. the ratio of RGM as measured
617 by either the UNR speciation systems or the 2P-LIF system divided by the value reported by the DOHGS
618 system. These values are typically much lower than those predicted by the McClure recovery expression. In
619 addition, on September 13th and for most of the 14th the 2P-LIF pyrolysis system sees little or no evidence
620 for high spike concentrations of HgBr₂ but records levels that fluctuate around those reported by the
621 speciation systems. The one exception is the spike at hour 18 on September 14th.

622 We suggest that the ability of the 2P-LIF pyrolysis system to monitor large spike concentrations is
623 shown by the measurements during the September 14th HgBr₂ spike at hour 18. The evidence for an
624 enhancement in the pyrolyzed sample stream is observable in the raw 7s averaged data and becomes clear
625 taking 5 minute averages. The absolute value of the pyrolyzed enhancement is obtained relative to the



626 concentration of the Hg(0) during the spike taken from the measurements by the UNR Tekran that are in
627 excellent agreement with the DOHGS Hg(0) values. The 2P-LIF measurements show a significantly larger
628 HgBr₂ concentration and a different temporal profile compared with the DOHGS instrument. In particular,
629 it is very difficult to rationalize the difference between the 2P-LIF and DOHGS systems during the first
630 hour of the spike. We would suggest it is difficult to make the case that both instruments are measuring the
631 same species. It is clear that the 2P-LIF pyrolyzer is operating efficiently based on the clear observation of
632 TOM at the end of the spike. We again note that the 2P-LIF system is not sensitive to TOM. It is important
633 to note that the DOHGS instrument requires an inline RGM scrubber to remove RGM before the
634 measurement of Hg(0). This inline scrubber utilizes deposition on uncoated quartz wool and the results of
635 Ambrose et al. (2013) imply that while uncoated quartz captures RGM efficiently in the presence of O₃,
636 quartz with a KCl coating promotes efficient reduction to Hg(0).

637 It is also reasonable to question the extent to which the Tekran speciation systems operated at
638 RAMIX reflect the performance of these systems when normally operated under protocols. As noted
639 above, the operation of the RAMIX manifold and the Tekran speciation systems has been questioned by
640 Prestbo (2014). In our view the two most significant issues are the performance of the two 2537 mercury
641 analyzers associated with each speciation system and the reduced sampling rate. The performance of the
642 two 2537 units is detailed in Gustin et al. (2013) and, as they noted, there was a significant response in each
643 instrument. Examination of Fig SI 6 of Gustin et al. (2013) shows the relative responses of the two
644 instruments and, using concentrations up to 25 ng m⁻³ i.e. manifold spikes, they list a regression of 0.72
645 [Hg(0)] + 0.08 whereas for the non-spike data they obtain 0.62[Hg(0)] + 0.25. Their Table SI 5 lists the
646 regression including spikes as 0.7 (±0.01) + 0.2, with all concentrations expressed in ng m⁻³. When
647 considering the use of these analyzers to monitor oxidized mercury the important factor to consider is the
648 loading on the gold cartridge. Table SI 3 lists the mean RGM concentrations from manifold sampling as 52
649 pg m⁻³ for SPEC1 and 56 pg m⁻³ for SPEC2. For a 1 hour sample at 4 L min⁻¹ this corresponds to a cartridge
650 loading of 13 pg. This is similar to the cartridge loading for sampling a concentration of 0.6 ng m⁻³ at 4 l
651 min⁻¹ for 5 minutes. If we examine Fig SI 6 of Gustin et al. (2013) we see that the regression analyses are
652 based on higher concentrations than 0.6 ng m⁻³, i.e. higher cartridge loadings. At concentrations of 0.6 ng
653 m⁻³ the ratio of SPEC2:SPEC1 obtained from these regressions would be 1.05, 0.85 and 1.06 depending on
654 which regression formula is used. We should note that based on Table SI 6 the median RGM
655 concentrations in manifold sampling were 41 and 46 pg m⁻³. The RGM concentrations for free standing
656 sampling were even lower with means of 26 and 19 pg m⁻³ and medians of 23 and 14 pg m⁻³ for SPEC1
657 and SPEC2 respectively. For concentrations below 40 pg m⁻³ the cartridge loading drops below 10 pg and
658 in addition, the Tekran 2537 integration routine becomes significant. Swartzendruber et al. (2009) reported
659 issues with the standard integration routine and note that below cartridge loadings of 10 pg the internal
660 integration routine produces a low bias in the Hg(0) concentration. They recommend downloading the raw
661 data, i.e. PMT output and integrating offline. This issue has recently been discussed by Slemr et al. (2016)
662 in a reanalysis of data from the CARIBIC program. This compounds the problem of correcting the bias



663 between SPEC1 and SPEC2. Because the speciation instruments were sampling at 4 L/min rather than the
664 recommended 10 L/min a large number the measurements made by the speciation systems are based on
665 uncorrected cartridge loadings of less than 10 pg m^{-3} . Based on the above we caution against drawing
666 significant conclusions based on differences between SPEC1 and the corrected SPEC2. These differences
667 are the basis of the conclusions of Gustin et al. (2013) that “On the basis of collective assessment of the
668 data, we hypothesize that reactions forming RM (reactive mercury) were occurring in the manifold”
669 (Gustin et al. (2013) abstract). Later they state “The same two denuders, coated by the same operator, were
670 used from Sept 2 to 13, and these were switched between instruments on September 9. Prior to switching
671 the slope for the equation comparing GOM as measured by Spec 1 versus Spec 2 adjusted was 1.7
672 ($r^2=0.57$, $p<0.5$, $n=76$) after switching this was 1.2 ($r^2=0.62$, $p<0.05$, $n=42$). This indicates that although
673 there may have been some systematic bias between denuders SPEC 2 adjusted consistently measured more
674 GOM than SPEC 1. We hypothesize that this trend is due to production of RM in the manifold (discussed
675 later).” If reactions in the manifold were producing RM then this production would surely have resulted in
676 the DOHGS measuring artificially high, i.e. higher than ambient, concentrations of oxidized mercury.
677 However, the paper by Ambrose et al. (2013) (written by a subset of the authors of Gustin et al.(2013))
678 makes no mention of manifold production of oxidized mercury. In fact Ambose et al. (2013) state, in the
679 supplementary information to their paper, “The same two denuders, prepared by the same operator, were
680 used in the Tekran® Hg speciation systems from 2 to 13 September. The denuders were switched between
681 Spec. 1 and Spec. 2 on 9 September. From 2 to 9 September, the Spec. 1-GOM/Spec. 2-GOM linear
682 regression slope was 1.7 ($r^2 = 0.57$; $p < 0.05$; $n = 76$); from 9 to 13 September the Spec. 1-GOM/Spec. 2-
683 GOM slope was 1.2 ($r^2 = 0.62$; $p < 0.05$; $n = 42$). These results suggest that the precisions of the GOM
684 measurements made with Spec. 1 and Spec. 2 were limited largely by inconsistent denuder performance.”

685 The oxidized mercury concentrations presented by Ambrose et al. (2013) for the RAMIX
686 measurements suggests a well-defined diurnal profile that peaks at night. It is important to note that the
687 error bars on this profile (Figure 3 of Ambrose et al.) are one standard error rather than one standard
688 deviation. The standard deviations, which actually give an indication of the range of concentrations
689 measured show much larger errors indicating significant day to day variation in these profiles.
690 Nevertheless, the measurements show much larger oxidized mercury concentrations than the speciation
691 systems and the very limited number of 2P-LIF measurements. As we note below, there is no known or
692 hypothesized chemistry that can reasonably explain the large RGM concentrations seen by the DOHGS
693 instrument. Both Gustin et al. (2013) and Ambrose et al. (2013) draw some conclusions about the chemistry
694 of mercury that have significant implications for atmospheric cycling. Gustin et al. suggest in their abstract
695 that “On the basis of collective assessment of the data, we hypothesize that reactions forming RM were
696 occurring in the manifold.” Later in a section on “Implications” they conclude “The lack of recovery of the
697 HgBr₂ spike suggests manifold reactions were removing this form before reaching the instruments.” The
698 residence time in the RAMIX manifold was on the order of 1s depending on sampling point and there is no
699 known chemistry that can account for oxidation of Hg(0) or reduction of RGM on this timescale. We would



700 suggest that the most reasonable explanation of the discrepancies between the various RAMIX
701 measurements includes both instrumental artifacts and an incomplete characterization of the RAMIX
702 manifold. If fast gas-phase chemistry is producing or removing RGM in the RAMIX manifold the same
703 chemistry must be operative in the atmosphere as a whole and this requires that we completely revise our
704 current understanding of mercury chemistry. The discrepancies between the DOHGS and speciation
705 systems are further indication that artifacts are associated with KCl denuder sampling under ambient
706 conditions but we would suggest that RAMIX does not constitute an independent verification of the
707 DOHGS performance and that the 2P-LIF measurements raise questions about the DOHGS measurements.
708 Ambrose et al. (2013) also suggest that the observations of very high RGM concentrations indicate
709 multiple forms of RGM and that the concentrations can be explained by oxidation of Hg(0), with O₃ and
710 NO₃ being the likely nighttime oxidants. We have discussed these reactions in detail previously (Hynes et
711 al., 2009) and concluded that they cannot play any role in homogeneous gas phase oxidation of Hg(0).
712 Ambrose et al. (2013) cite recent work on this reaction by Rutter et al. (2012) stating that “On the basis of
713 thermodynamic data for proposed reaction mechanisms, purely gas-phase Hg(0) oxidation by either O₃ or
714 NO₃ is expected to be negligibly slow under atmospheric conditions; however, in the case of O₃-initiated
715 Hg(0) oxidation, the results of laboratory kinetics studies unanimously suggest the existence of a gas-phase
716 mechanism for which the kinetics can be treated as second-order.” We would suggest that a careful reading
717 of the cited work by Rutter et al. (2013) demonstrates the opposite conclusion. We provide additional
718 discussion of these issues in the SI and again conclude that O₃ and NO₃ can play no role in the
719 homogeneous gas phase oxidation of Hg(0).

720

721 **5.0 Future Mercury Intercomparisons:**

722 The discrepancies that are discussed above suggest a need for a careful independent evaluation of
723 mercury measurement techniques. The approaches used during the evaluation of instrumentation for the
724 NASA Global Tropospheric Experiment (GTE) and the Gas-Phase Sulfur Intercomparison Experiment
725 (GASIE) evaluation offer good models for such an evaluation. The Chemical Instrument and Testing
726 Experiments (CITE 1-3) (Beck et al., 1987; Hoell et al., 1990; Hoell et al., 1993) were a major component
727 of GTE establishing the validity of the airborne measurement techniques used in the campaign. The GASIE
728 experiment (Luther and Stetcher, 1997; Stetcher et al., 1997) was a ground based intercomparison of SO₂
729 measurement techniques that might be particularly relevant to issues associated with mercury measurement.
730 In particular, GASIE was a rigorously blind intercomparison that was overseen by an independent panel
731 consisting of three atmospheric scientists none of whom were involved in SO₂ research. We would suggest
732 that a future mercury intercomparison should be blind with independent oversight. Based on the RAMIX
733 results it should consist of a period of direct ambient sampling and then manifold sampling in both reactive
734 and unreactive configurations. For example an unreactive configuration would consist of Hg(0) and
735 oxidized mercury in an N₂ diluent eliminating any possibility of manifold reactions and offering the
736 possibility of obtaining a manifold blank response. Such a configuration would allow the use of both



737 denuder and pyrolysis measurements since it is reasonable to conclude, based on the current body of
738 experimental evidence, that denuder artifacts are associated with ambient sampling with water vapor and
739 ozone as the most likely culprits. A reactive configuration would be similar to the RAMIX manifold
740 configuration with atmospheric sampling into the manifold and periodic addition of Hg(0) and oxidized
741 mercury over their ambient concentrations. The combination of the three sampling configurations should
742 enable instrumental artifacts to be distinguished from reactive chemistry in either the manifold itself or, for
743 example, on the KCl denuder.

744 **6.0 Conclusions**

745 We deployed a 2P-LIF instrument for the measurement of Hg(0) and RGM during the RAMIX campaign.
746 The Hg(0) measurements agreed reasonably well with instruments using gold amalgamation sampling
747 coupled with CVAFS analysis of Hg(0). Measurements agreed to 10-25% on the short term variability in
748 Hg(0) concentrations based on a 5 minute temporal resolution. Our results also suggest that the operation of
749 the RAMIX manifold and spiking systems were not as well characterized as Finley et al. (2013) suggest.
750 We find that the calculated concentration spikes consistently overestimated the amount of Hg(0) introduced
751 into the RAMIX manifold by as much as 30%. This suggests a systematic error in concentration
752 calculations rather than random uncertainties that should not produce a high or low bias.

753 We made measurements of TGM, and hence TOM by difference, by using pyrolysis to convert
754 TOM to Hg(0) and switching between pyrolyzed and ambient samples. The short term variation in ambient
755 Hg(0) concentrations is a significant limitation on detection sensitivity and suggests that a two channel
756 detection system, monitoring both the pyrolyzed and ambient channels simultaneously is necessary for
757 ambient TOM measurements. Our TOM measurements were normally consistent, within the large
758 uncertainty, with KCl denuder measurements obtained with two Tekran Speciation Systems and with our
759 own manual KCl denuder measurements. The ability of the pyrolysis system to measure higher RGM
760 concentrations was demonstrated during one of the manifold HgBr₂ spikes but the results did not agree with
761 those reported by the UW DOHGS system. We would suggest that it is not possible to reconcile the
762 different measurement approaches to TOM. While there is other evidence that KCl denuders may
763 experience artifacts in the presence of water vapor and ozone the reported discrepancies cannot explain the
764 very large differences reported by the DOHGS and Tekran speciation systems. Similarly, the differences
765 between the DOHGS and 2P-LIF pyrolysis measurements suggest that one or both of the instruments were
766 not making reliable, quantitative measurements of RGM. We suggest that both instrumental artifacts, an
767 incomplete characterization of the sampling manifold, and limitations in the measurement protocols make
768 significant contributions to the discrepancies between the different instruments and that it would be rash to
769 draw significant implications for the atmospheric cycling of mercury based on the RAMIX results. This is
770 particularly true of the RGM results. If one were to conclude that the discrepancies between the DOHGS
771 and speciation systems sampling ambient oxidized mercury are accurate and reflect a bias that can be
772 extrapolated to global measurements then it means that atmospheric RGM concentrations are much higher
773 than previously thought and that we have little understanding of the atmospheric cycling of mercury. What



774 is not in dispute is the urgent need to resolve the discrepancies between the various measurement
775 techniques. The RAMIX campaign provided a valuable guide for the format of any future mercury
776 intercomparison. It clearly demonstrated the need to deploy high accuracy calibration sources of Hg(0) and
777 oxidized mercury, the need for multiple independent methods to measure elemental and oxidized mercury
778 and to clearly characterize and understand the differences reported by instruments that are currently being
779 deployed for measurements.

780

781 **Acknowledgements**

782 This work was supported by NSF Grant # AGS-1101965, a National Science Foundation Major
783 Instrumental Grant (#MRI-0821174) and by the Electric Power Research Institute. We thank Mae Gustin
784 and her research group and Dr Robert Novak for their hospitality, assistance and use of laboratory facilities
785 during the RAMIX intercomparison. We thank Mae Gustin and Dan Jaffe for the use of their RAMIX data
786 for comparison with our results. We thank Eric Prestbo for helpful comments on the manuscript.

787

788

789 **References:**

790 Ambrose, J. L.; Lyman, S. N.; Huang, J.; Gustin, M. S.; Jaffe, D. A.: Fast time resolution oxidized mercury
791 measurements during the Reno Atmospheric Mercury Intercomparison Experiment (RAMIX), Environ.
792 Sci. Technol., 47 (13), 7284–7294; DOI 10.1021/es303916v, 2013.

793

794 Bauer, D.; Campuzano-Jost, P.; Hynes, A. J., Rapid, ultra-sensitive detection of gas phase elemental
795 mercury under atmospheric conditions using sequential two-photon laser induced fluorescence, J. Environ.
796 Monitor., 4, (3), 339-343, 2002.

797

798 Bauer, D., D'Ottone, L., Campuzano-Jost, P. and Hynes, A. J.: Gas Phase
799 Elemental Mercury: A Comparison of LIF Detection Techniques and
800 Study of the Kinetics of Reaction with the Hydroxyl Radical, J. Photochem.
801 Photobio, 57, 247, 2003

802

803 Bauer, D., Everhart, S., Remeika, J., Tatum Ernest, C., and Hynes, A. J.: Deployment of a Sequential Two-
804 Photon Laser Induced Fluorescence Sensor for the Detection of Gaseous Elemental Mercury at Ambient
805 Levels: Fast, Specific, Ultrasensitive Detection with Parts-Per-Quadrillion Sensitivity, Atmos. Meas.
806 Tech., 7, 4251-4265, www.atmos-meas-tech-discuss.net/7/5651/2014/ doi:10.5194/amtd-7-5651-2014,
807 2014.

808



- 809 Breckenridge, W. H. and Umemoto, H.: Collisional Quenching of Electronically Excited Metal Atoms, in
810 Advances in Chemical Physics: Dynamics of the Excited State, Volume 50 (ed K. P. Lawley), John Wiley
811 & Sons, Inc., Hoboken, NJ, USA. doi: 10.1002/9780470142745.ch5, 2007.
- 812
- 813 Beck, S. M.; Bendura, R. J.; Mcdougal, D. S.; et al.: Operational overview of NASA GTE CITE-1 airborne
814 instrument intercomparisons - carbon-monoxide, nitric-oxide, and hydroxyl instrumentation, J. Geophys.
815 Res., 92, 1977-1985, 1987
- 816
- 817 Diez, S.: Human health effects of methylmercury exposure, Rev. Environ. Contam. Toxicol., 198,
818 111–132, DOI: 10.1007/978-0-387-09646-9, 2009.
- 819
- 820 Ebinghaus, R.; Banic, C.; Beauchamp, S.; Jaffe, D.; Kock, H.; Pirrone, N.; Poissant, L.; Sprovieri, F.;
821 Weiss-Penzias, P., Spatial coverage and temporal trends of land-based atmospheric mercury measurements
822 in the Northern and Southern Hemispheres. In Mercury fate and transport in the global atmosphere:
823 Emissions, measurements and models, Mason, R.; Pirrone, N., Eds. Springer: New York, NY, 2009.
- 824
- 825 Ernest, C.T.; Donohoue, D.; Bauer, D.; Ter Schure, A.; Hynes, A.J. Programmable Thermal Dissociation of
826 Reactive Gaseous Mercury, a Potential Approach to Chemical Speciation: Results from a Field Study,
827 Atmosphere, 5, 575-596. doi:[10.3390/atmos5030575](https://doi.org/10.3390/atmos5030575), 2014
- 828
- 829 Feng, X.; Lu, J.; Gregoire, D. C.; Hao, Y.; Banic, C. M.; Schroeder, W. H. : Analysis of inorganic mercury
830 species associated with airborne particulate matter/aerosols: Method development, Anal. Bioanal. Chem.,
831 380, 683–689, 2004.
- 832
- 833 Finley, B. D.; Jaffe, D. A.; Call, K.; Lyman, S.; Gustin, M.; Peterson, C.; Miller, M.; Lyman, T. :
834 Development, testing, and deployment of an air sampling manifold for spiking elemental and oxidized
835 mercury during the Reno Atmospheric Mercury Intercomparison Experiment (RAMIX). Environ. Sci.
836 Technol., 44, 7277-7284,
837 DOI 10.1021/es304185a, 2013
- 838
- 839 Gustin, M.; Jaffe, D., Reducing the Uncertainty in Measurement and Understanding of Mercury in the
840 Atmosphere. Environ. Sci. Technol., 44, (7), 2222-2227, 2010.
- 841
- 842 Gustin, M. S.; Huang, J.; Miller, M. B.; Peterson, C.; Jaffe, D. A.; Ambrose, J.; Finley, B. D.; Lyman, S.
843 N.; Call, K.; Talbot, R.; Feddersen, D.; Mao, H.; Lindberg, S. E. Do we understand what the mercury
844 speciation instruments are actually measuring? Results of RAMIX. Environ. Sci. Technol., 47 (13), 7295–
845 7306; DOI 10.1021/es3039104, 2013.



- 846
- 847 Hoell, J. M. ; Albritton, D. L.; Gregory, G. L.; et al., Operational overview of NASA GTE/CITE-2 airborne
848 instrument intercomparisons - nitrogen-dioxide, nitric-acid, and peroxyacetyl nitrate, *J. Geophys. Res.*, 95
849 10047-10054, 1990
- 850
- 851 Hoell, J. M. ; Davis, D. D.; Gregory, G. L.; et al., operational overview of the NASA GTE CITE-3 airborne
852 instrument intercomparisons for sulfur-dioxide, hydrogen-sulfide, carbonyl sulfide, dimethyl sulfide, and
853 carbon-disulfide, *J. Geophys. Res.*, 98, 23291-23304, 1993.
- 854
- 855 Houyoux, M.; Strum, M. Memorandum: Emissions Overview: Hazardous Air Pollutants in Support of the
856 Final Mercury and Air Toxics Standard; EPA-454/R-11-014; Emission Inventory and Analysis Group Air
857 Quality Assessment Division: Research Triangle Park, NC, USA, 2011.
- 858 Available at: <http://www.epa.gov/mats/pdfs/20111216EmissionsOverviewMemo.pdf>
- 859
- 860 Hynes, A. J.; Donohoue, D. L.; Goodsite, M. E.; Hedgecock, I. M., Our current understanding of major
861 chemical and physical processes affecting mercury dynamics in the atmosphere and at the air-
862 water/terrestrial interfaces In *Mercury Fate and Transport in the Global Atmosphere*, Mason, R.; Pirrone,
863 N., Eds. Spring New York, NY, 2009.
- 864
- 865 Landis, M. S.; Stevens, R. K.; Schaedlich, F.; Prestbo, E. M., Development and Characterization of an
866 Annular Denuder Methodology for the Measurement of Divalent Inorganic Reactive Gaseous Mercury in
867 Ambient Air. *Environ. Sci. Technol.*, 36, (13), 3000-3009, 2002.
- 868
- 869 Lin, C.J.; Pongprueksa, P.; Lindberg, S.E.; Pehkonen, S.O.; Byun, D.; Jang, C. Scientific uncertainties in
870 atmospheric mercury models I: Model science evaluation. *Atmos. Environ.*, 40, 2911–2928,
871 doi:10.1016/j.atmosenv.2006.01.009, 2006.
- 872
- 873 Lindberg, S. E.; Bullock, R.; Ebinghaus, R.; Engstrom, D.; Feng, X.; Fitzgerald, W.; Pirrone, N.; Prestbo,
874 E.; Seigneur, C. A synthesis of progress and uncertainties in attributing the sources of mercury in
875 deposition. *Ambio*, 36, 1932, 2007.
- 876
- 877 Luther III, D. W.; D.L.; Stecher, H.A. III, Preface: Historical background. *J. Geophys. Res.*, 102, 16215-
878 16217, 1997.
- 879
- 880 Lyman, S. N.; Jaffe, D. A.; Gustin, M. S. Release of mercury halides from KCl denuders in the presence of
881 ozone. *Atmos. Chem. Phys.* 2010, 10, 8197–8204; DOI 10.5194/acp-10- 8197- 2010.



- 882 Mason, R.A. Mercury Emissions from Natural Processes and their Importance in the Global Mercury
883 Cycle. In Mercury Fate and Transport in the Global Atmosphere: Emissions, Measurements and Models;
884 Pirrone, N., Mason, R.A., Eds.; Springer: Dordrecht, The Netherlands, 2009; pp. 173–191.
885
886 Mergler, D.; Anderson, H.A.; Chan, L.H.M.; Mahaffey, K.R.; Murray, M.; Sakamoto, M.; Stern, A.H.
887 Methylmercury exposure and health effects in humans: A worldwide concern. *Ambio* 2007, 36, 3–11,
888 doi:10.1579/0044-7447(2007)
889
890 McClure, C. D.; Jaffe, D.A.; Edgerton, E.S. Evaluation of the KCl denuder method for gaseous oxidized
891 mercury using HgBr₂ at an in-service AMNet site. | *Environ. Sci. Technol.* 2014, 48, 11437–11444,
892 dx.doi.org/10.1021/es502545k
893
894 Prestbo, E. C., Air Mercury Speciation Accuracy and Calibration, SFO Air Mercury Speciation Workshop,
895 July 2014. Available at <http://omicsgroup.com/conferences/ACS/conference/pdfs/14958-Speaker-Pdf-T.pdf>
896
897 Prestbo, E. C., Chief Scientist, Tekran Instruments, personal communication, 2015.
898
899 Pirrone, N.; Cinnirella, S.; Feng, X.; Finkelman, R.B.; Friedli, H.R.; Learner, J.; Mason, R.; Mukherjee,
900 A.B.; Stracher, G.; Streets, D.G.; Telmer, K. Global mercury emissions to the atmosphere from natural and
901 anthropogenic sources. In Mercury Fate and Transport in the Global Atmosphere: Emissions,
902 Measurements and Models; Pirrone, N., Mason, R.A., Eds.; Springer: Dordrecht, The Netherlands, 2009;
903 pp. 3–50.
904
905 Rutter, A.P., Shakya, K.M., Lehr, r., Schauer, J. J., Griffin, R. J., Oxidation of gaseous elemental mercury
906 in the presence of secondary organic aerosols, *Atmos. Environ.*, 59, 86-92, 2012
907
908 Scheuhammer, A.M.; Meyer, M.W.; Sandheinrich, M.B.; Murray, M.W., Effects of environmental
909 methylmercury on the health of wild bird, mammals, and fish. *Ambio* 2007, 36, 12–18, doi:10.1579/0044-
910 7447(2007)36[12:EOEMOT]2.0.CO;2.
911
912 Selin, N.E., Global Biogeochemical Cycling of Mercury: A Review. *Annu. Rev. Environ. Resour.* 2009,
913 34, 43–63, doi:10.1146/annurev.environ.051308.084314.
914
915 Slemr, F., Brunke, E.-G., Ebinghaus, R., and Kuss, J.: Worldwide trend of atmospheric mercury since
916 1995, *Atmos. Chem. Phys.*, 11, 4779-4787, doi:10.5194/acp-11-4779-2011, 2011.
917



- 918 Slemr, F.; Weigelt, A.; Ebinghaus, R.; Kock, H.H.; Bödewadt, J.; Brenninkmeijer, C.A.M.; Rauthe-Schöch,
919 A.; Weber, S.; Hermann, M.; Zahn, A.; Martinsson, B.; Atmospheric mercury measurements onboard the
920 CARIBIC passenger aircraft, Atmos. Chem. Phys., accepted for publication, 2016
921
922 Sprovieri, F., Pirrone, N., Ebinghaus, R., Kock, H., and Dommergue, A.: A review of worldwide
923 atmospheric mercury measurements, Atmos. Chem. Phys., 10, 8245–8265, doi:10.5194/acp-10-8245-2010,
924 2010.
925
926 Streets, D.G.; Devane, M.K.; Lu, Z.; Bond, T.C.; Sunderland, E.M.; Jacob, D.J. All-time releases of
927 mercury to the atmosphere from human activities. Environ. Sci. Technol. 2011, 45, 10485–10491.
928
929 Stecher, H.A. III; Luther III, G.W.; MacTaggart, D.L.; Farwell, S.O.; Crossley, D.R.; Dorko, W.D.;
930 Goldan, P.D.; Beltz, N.; Kriskhke, U.; Luke, W.T.; Thornton, D.C.; Talbot, R.W.; Lefer, B.L.; Scheuer,
931 E.M.; Benner, R.L.; Wu, J.; Saltzman, E.S.; Gallagher, M.S.; Ferek, R.J.: Results of the gas- phase sulfur
932 intercomparison experiment (GASIE): Overview of experimental setup, results, and general conclusions, J.
933 Geophys. Res., 102, 16219-16236, 1997
934
935 Subir, M.; Ariya, P. A.; Dastoor, A. P., A review of uncertainties in atmospheric modeling of mercury
936 chemistry I. Uncertainties in existing kinetic parameters : Fundamental limitations and the importance of
937 heterogeneous chemistry. Atmos. Environ., 45, 5664-5676, 2011.
938
939 Subir, M.; Ariya, P.A.; Dastoor, A.P. A review of the sources of uncertainties in atmospheric mercury
940 modeling II. Mercury surface and heterogeneous chemistry—A missing link. Atmos. Environ. 2012, 46, 1–
941 10, doi:10.1016/j.atmosenv.2011.07.047.
942
943 Swartzendruber, P. C.; Jaffe, D. A.; Finley, B.: Improved fluorescence peak integration in the Tekran 2537
944 for applications with sub-optimal sample loadings, Atmos. Environ., Volume 43, 3648-3651, 2009
945
946 UNEP, United Nations Environment Program, Chemicals Branch, Mercury, Time to Act, 2013
947
948 UNEP, United Nations Environment Program, Chemicals Branch, The Global Atmospheric Mercury
949 Assessment: Sources, Emissions and Transport, 2008.
950
951 UNEP, United Nations Environment Program: <http://www.mercuryconvention.org>, 2014
952
953 U.S. EPA, United States Environmental Protection Agency “Mercury Research Strategy”, EPA/600/R-
954 00/073, , September 2000.



955

956 U.S. EPA, United States Environmental Protection Agency, [Mercury and Air Toxics Standard](#). Available957 [online: http://www.epa.gov/mats](http://www.epa.gov/mats) (accessed on 13 March 2013).

958

959

960

961

962

963 Table 1: RAMIX Manual KCl Denuder Sampling

Date	Sample time	mid point	sample	blank	time	spec1		spec2 (uncorr)	
	hours	hour	pg m ⁻³	pg m ⁻³		GOM	PBM	GOM	PBM
						pg m ⁻³	pg m ⁻³	pg m ⁻³	pg m ⁻³
9/6	1.5	15	127.9*	2.27	13:00	200.7	51.8	205.1	4.3
					15:00	65.7	32.0	84.9	6.0
9/7	2	16	112.9*	0	14:00	39.8	136.4	94.3	2.5
			21.2		16:00	48.5	177.3	68.9	1.5
			285.8*		18:00	28.1	182.2	37.4	3.3
			30.6						
9/10	3	15.3	74.3	1995	14:00	26.7	10.5	27.4	4.2
			44.2		16:00	24.1	18.3	23.7	2.3
9/13	4	15	12.8	8.2	13:00	0.7	16.9	0.5	16.6
			13.56		17:00	37.6	16.1	25.2	2.7
9/14	4.5	14	39*	3.3	12:00	34.9	12.0	23.9	5.5
			17.3		14:00	57.	18.4	26.3	38.6
					16:00	42.0	17.4	26.3	4.0
9/15	4.5	15	15.24	1.53	13:00	113.9	39.1	27.6	3.9
			20.4	4.87	15:00	80.6	22.2	17.7	3.9
					17:00	110.8	24.1	8.6	8.1



9/16	2.75	16	148*	5	8:00	19.7	4.7	14.8	5.4
			42	6	9:00				
			26	5	10:00	28.7	13.3	19.9	4.8
			47	4					

964 • * evidence from TDP's for presence of PBM

965 • Measurements for UNR Speciation system made at similar times. The Spec 2 measurements are
966 uncorrected values.

967

968

969

970

971

972

973

974

975

976

977

978

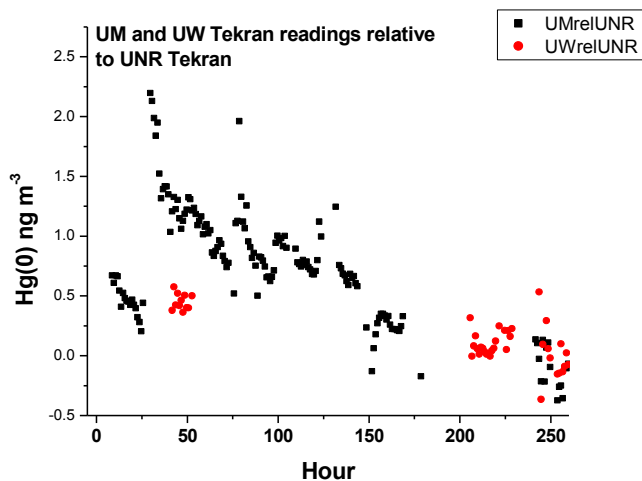
979

980

981

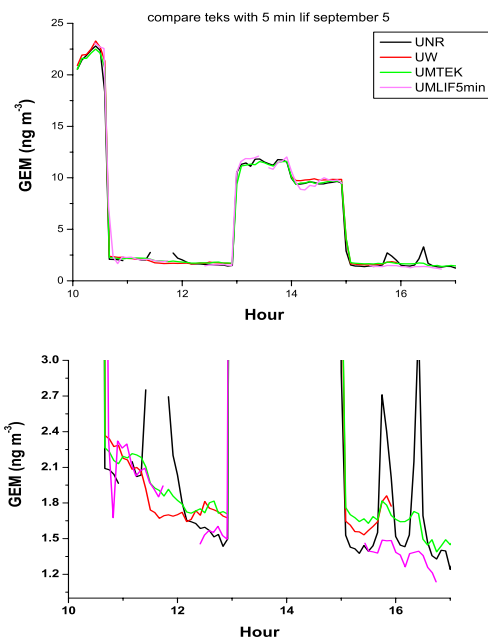
982

983 **Figures.**



984

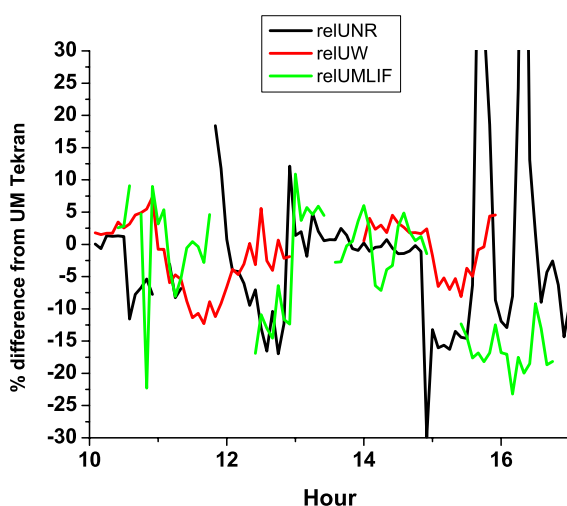
985 Figure 1. Comparison of Hg(0) readings from the UM, UW and UNR Tekrans over the first 260 hours of
986 UM measurements. The absolute concentration difference relative to the UNR instrument is shown in black
987 for the UM Tekran and in red for the DOHGS (UW) Tekran.



988

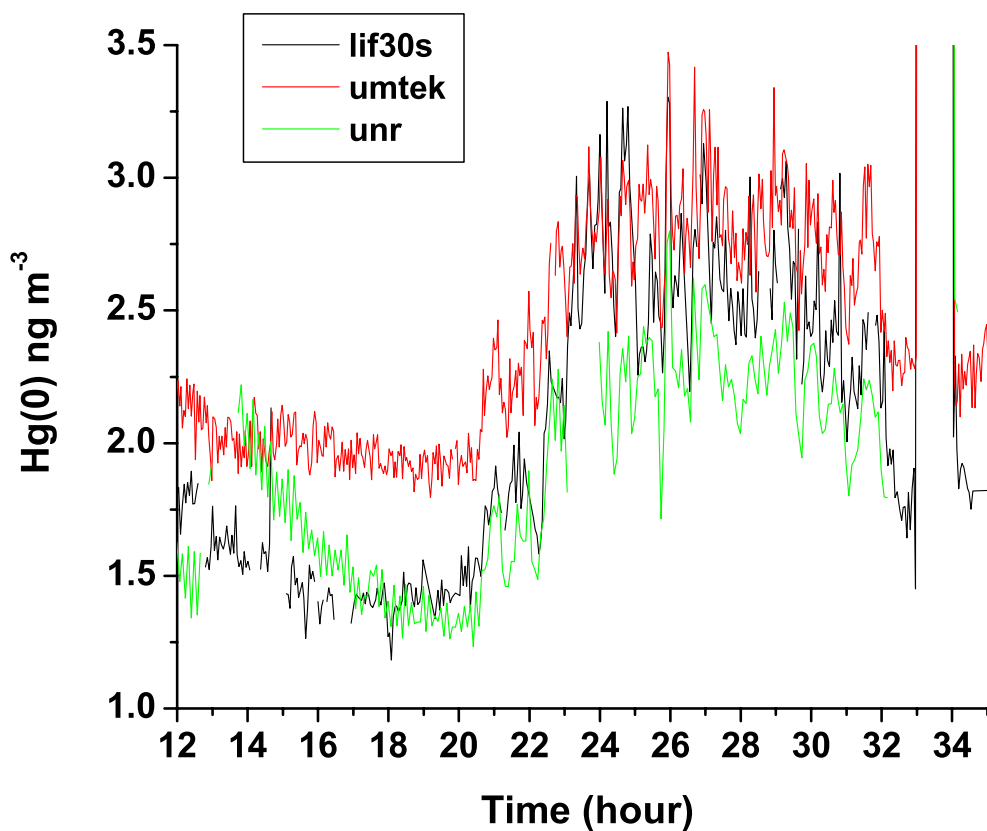


989 Figure 2: a). A seven hour sequence of GEM measurements from September 5th that included two manifold
990 spikes. Shown are the sequence of GEM measurements from the UNR, UW and UM Tekrans together with
991 the 5 minute averages of the 2P-LIF signal. b) An expanded concentration scale focusing on ambient
992 measurements.
993
994



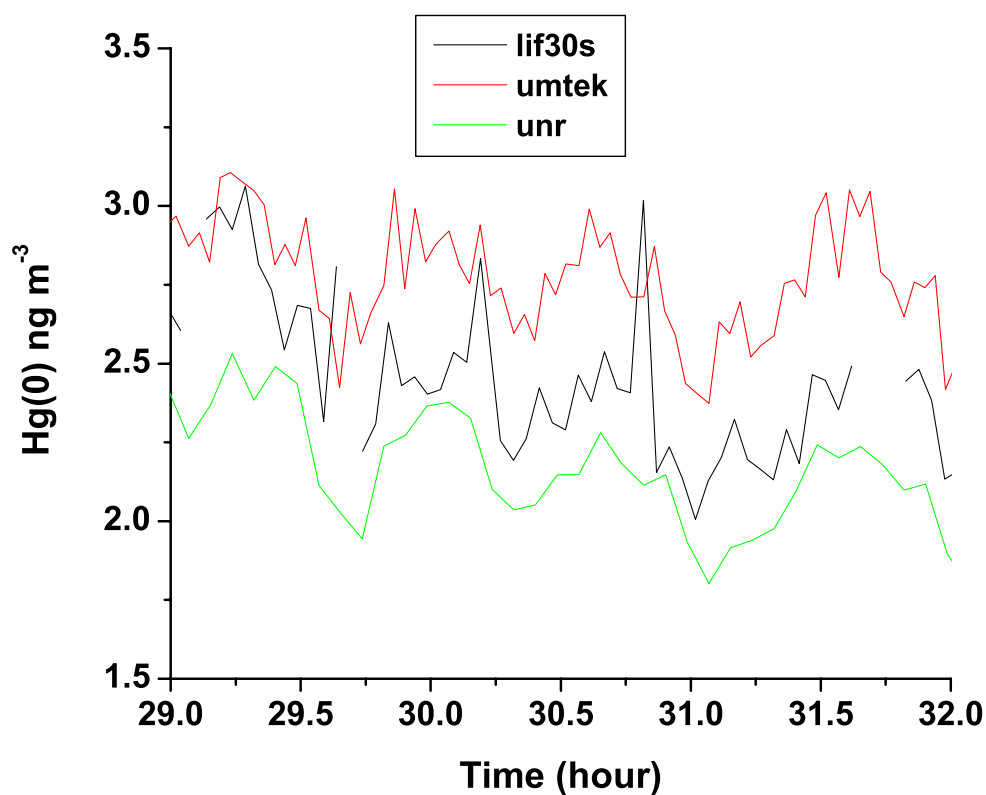
995
996
997 Figure 3: Seven hour measurement period from September 5th. The % difference of the UNR (black line)
998 and UW (red line) Tekrans and the UM 2P-LIF (blue line) measurements relative to the UM Tekran is
999 shown.

1000
1001
1002
1003
1004
1005
1006
1007
1008
1009
1010
1011



1012
1013
1014
1015
1016
1017
1018
1019
1020
1021
1022
1023
1024
1025

Fig 4: 22 hour sampling period from September 1st and 2nd. Comparison of the UM (red line) and UNR (green line) Tekrans with the UM 2P-LIF (black line) concentrations. The concentrations for each instrument are scaled to force agreement during the second manifold spike at hour 33. This is the data from SI Fig. 3 with the concentration scale expanded to shown only ambient data.



1026

1027

1028

1029

1030

1031 Fig 5: A section of the 22 hour sampling period from September 1st and 2nd. Comparison of the UM (red

1032 line) and UNR (green line) Tekrans with the UM 2P-LIF (black line) concentrations. The concentrations

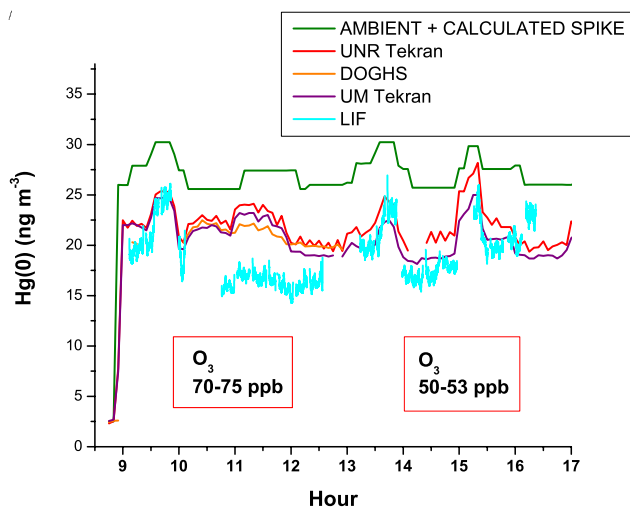
1033 for each instrument are scaled to force agreement during the second manifold spike at hour 33. This is the

1034 data from SI Fig. 3 with the concentration scale expanded to shown only ambient data between hours 29

1035 and 32.

1036

1037



1038

1039

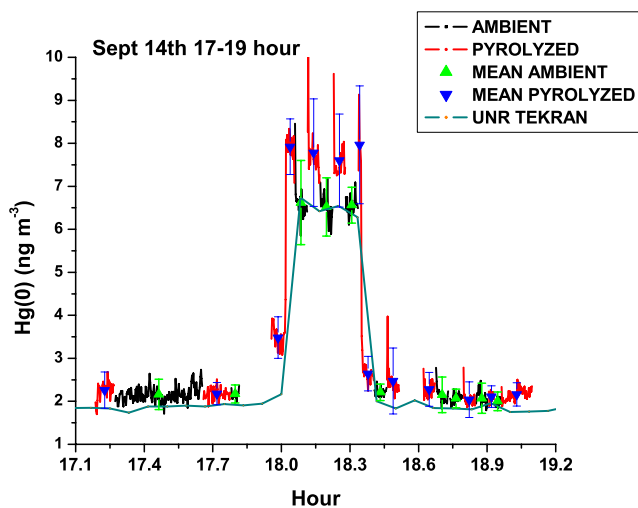
1040 Figure 6: September 7th an ozone interference test. A comparison of the UM, UW and UNR Tekrans and

1041 the UM-2P-LIF measurements. The “expected” concentration calculated from the ambient Hg(0)

1042 concentration prior to the spike plus the calculated spike concentration is also shown.

1043

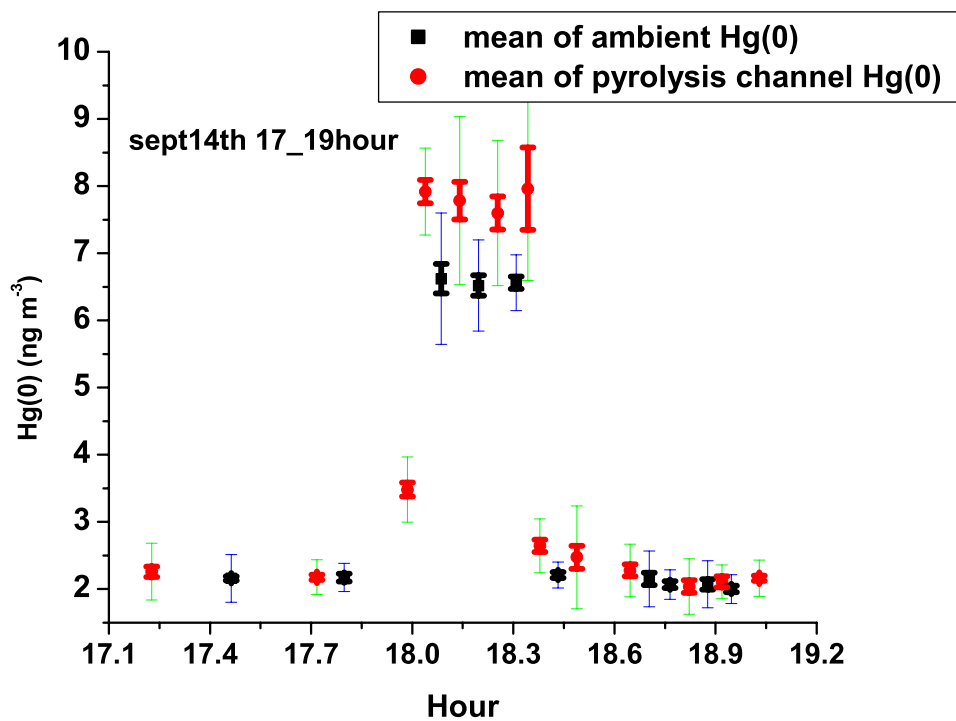
1044



1045

1046

1047 Fig 7: September 14 measurements hours 17-19 (5-7pm). The background subtracted 2P-LIF signals from
1048 the ambient (black) and pyrolyzed sampling lines (red) are shown. The gaps correspond to times when the
1049 laser was blocked to check power and background. The means and 1 standard deviation of each sample are
1050 shown. The absolute Hg(0) concentrations are obtained by scaling the ambient Hg(0) signal to the absolute
1051 Hg(0) concentration reported by the UNR Tekran during the Hg(0) manifold spike.
1052



1053

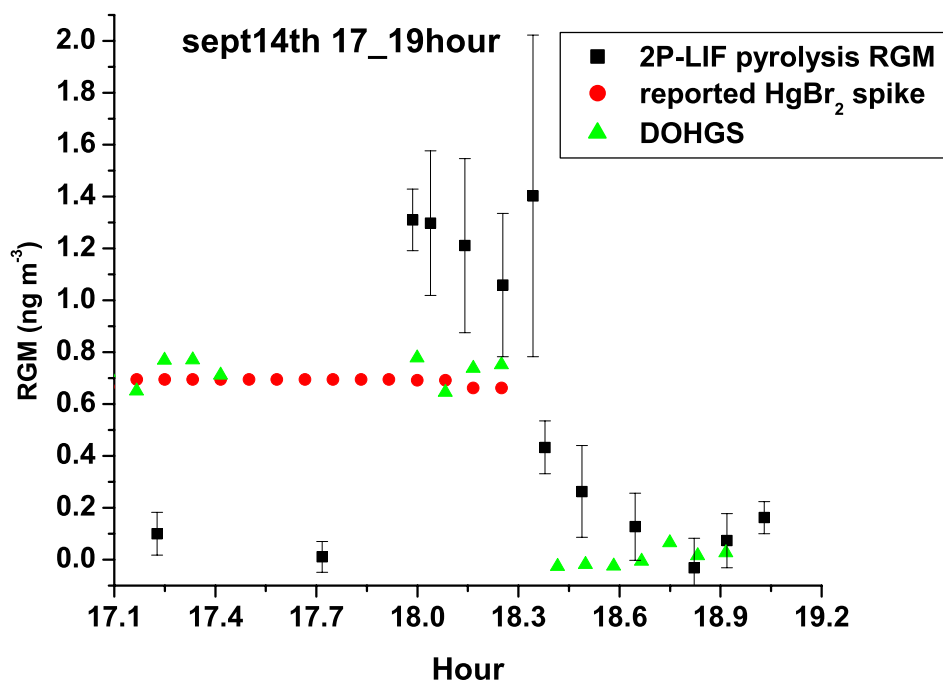
1054

1055 Fig. 8: September 14 measurements hour 17-19. The means of the ambient channel (black) and pyrolyzed

1056 channel (red) are shown. The error bars show both 2 standard errors (thicker line) and 2 standard

1057 deviations.

1058



1059

1060

1061 Fig 9: TOM concentrations calculated from the difference between the pyrolyzed and ambient sample

1062 concentrations together with 2SE in the TOM concentrations. The reported HgBr₂ spike concentrations and

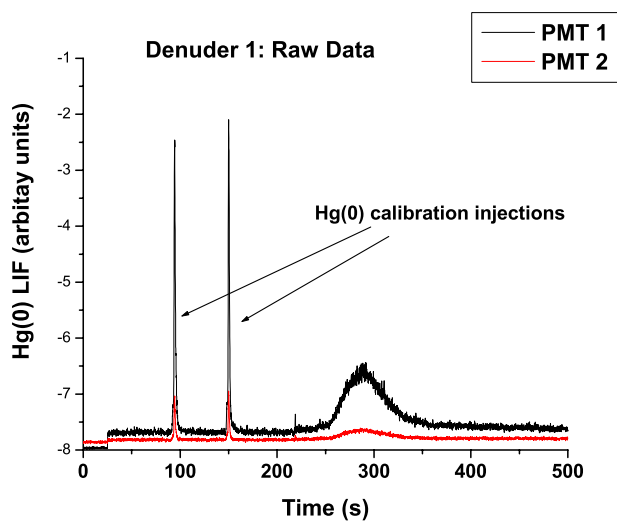
1063 DOHGS measurements are also shown.

1064

1065



1066



1067

1068

1069 Fig. 10: September 16th KCl manual denuder measurements. The raw data for the temporal decomposition
1070 profiles (TDP) for the denuder D1 is shown.

1071

1072

1073

1074

1075

1076

1077

1078

1079

1080

1081

1082

1083

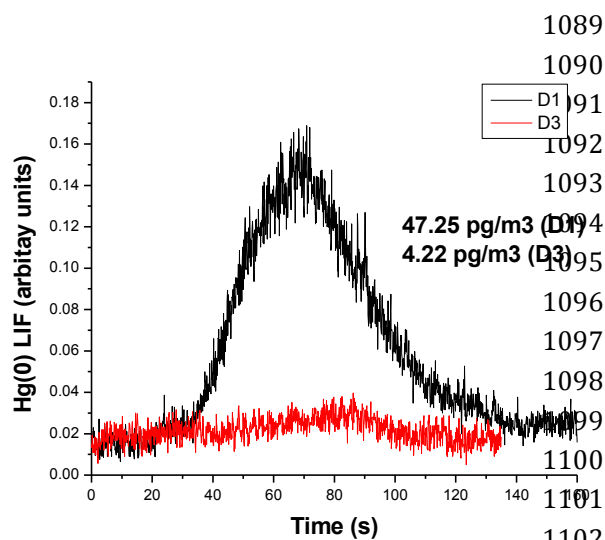
1084

1085

1086

1087

1088



1089
1090
1091
1092
1093
1094
1095
1096
1097
1098
1099
1100
1101
1102
1103
1104

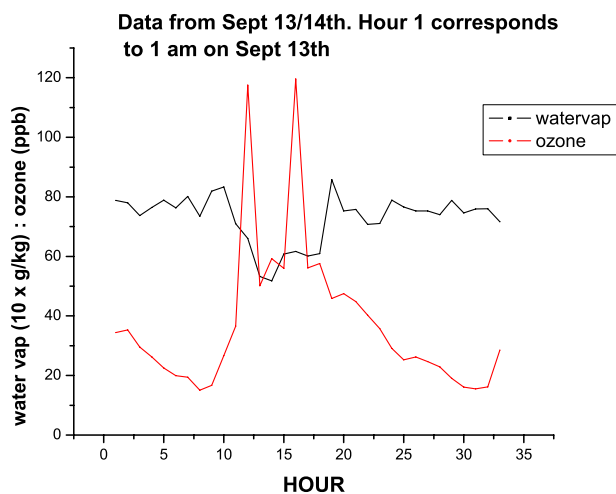
Fig. 11 September
16th KCl manual

1105 denuder measurements. The calibrated temporal decomposition profiles (TDP) for the tandem denuder pair,
1106 D1 and D3 are shown.

1107
1108
1109
1110
1111
1112
1113
1114
1115
1116
1117
1118
1119
1120
1121
1122
1123
1124
1125



1126



1127

1128

1129

1130 Fig. 12: The ozone concentration and absolute humidity for a 35 hour sampling period on September 13th

1131 and 14th that included two ozone spikes and only sampled ambient TOM.

1132

1133

1134

1135

1136

1137

1138

1139

1140

1141

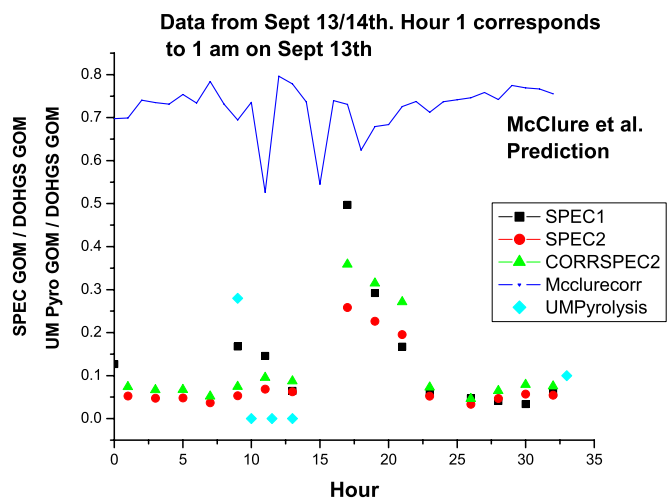
1142

1143

1144

1145

1146



1147

1148

1149 Fig. 13. Expected denuder recovery based on the formula determined by McClure et al. which varies
1150 between a typical value of ~70% dropping to ~50% during the ozone spikes. The figure also shows the
1151 reported recoveries i.e. the ratio of RGM as measured by either the UNR speciation systems or the 2P-LIF
1152 system divided by the value reported by the DOHGS system.

1153

1154

1155

1156

1157

1158

1159

1160

1161

1162

1163

1164

1165

1166

1167

1168

1169

1170